Strong IP anomalies with P.F.E. of more than 3.0% are found in the Block South in the form of a band, and increase those distribution area to the depth.

1) n=1 (Fig. II–3–15)

At the Block North, P.F.E. values of less than 2.0%, thought to be background values in this survey area, are widely distributed, and only one IP anomaly with N-S trend is found at the central part.

At the Block South, two IP anomalies are detected at the western part and at the central part. The central IP anomaly is distributed in a direction of NNE-SSW, and local strong IP indications of more than 4.0% is found at the central portion of the western anomaly with N-S trend.

2) n=3 (Fig. II–3–16)

At the Block North, IP anomalies, extending towards south beyond the survey area, are widely distributed at the southern part from Line 130S, and suggest the existence of bload IP anomalous body at deeper part than −100 mGL.

At the Block South, two IP anomalies are found at the western part and at the central to eastern part. The western IP anomaly occupies larger distribution area than that on the n=1 map, and in this anomaly, P.F.E. values of more than 4.0% are found at the southern part from Line 310S and show N-S trend.

3) n=5 (Fig. II–3–17)

At the Block North, IP anomalies increase those distribution area and those P.F.E. values towards south. At the Block South, distribution of IP anomalies are almost same as those on the n=1 and 3 maps. But the center of the anomaly shifts to the central part of the block comparing to the n=1 and 3 maps, because IP anomalous source causing this IP anomaly may dip to the east.

3–1–3 *Spectrum Diagram*

Utilizing the EM-decoupled values for a part of the observed data, spectrum diagrams for phase-difference, Cole-Cole, and magnitude were made. Phase-difference spectrum diagrams are shown in Fig. II–3–18 and Fig. II–3–19, magnitude diagrams in Fig. II–3–20 and Fig. II–3–21, and Cole-Cole diagrams in Fig. II–3–22 and Fig. II–3–23.

Four kind of remarkable spectral patterns could be found in each spectrum diagram, and are called Types A, B, C and D, shown in Fig. II–3–24. Within those, Types A and B show similar pattern as that caused by sulfide minerals. However, the spectral patterns obtained in this survey seem not to be due to one kind of rock and/or one kind of mineral and to be caused by the assembly of several rocks and/or minerals, so it is very difficult to discriminate minerals from spectral pattern only. The qualitative interpretation for four types of spectral patterns are given

PALMEIRÓPOLIS

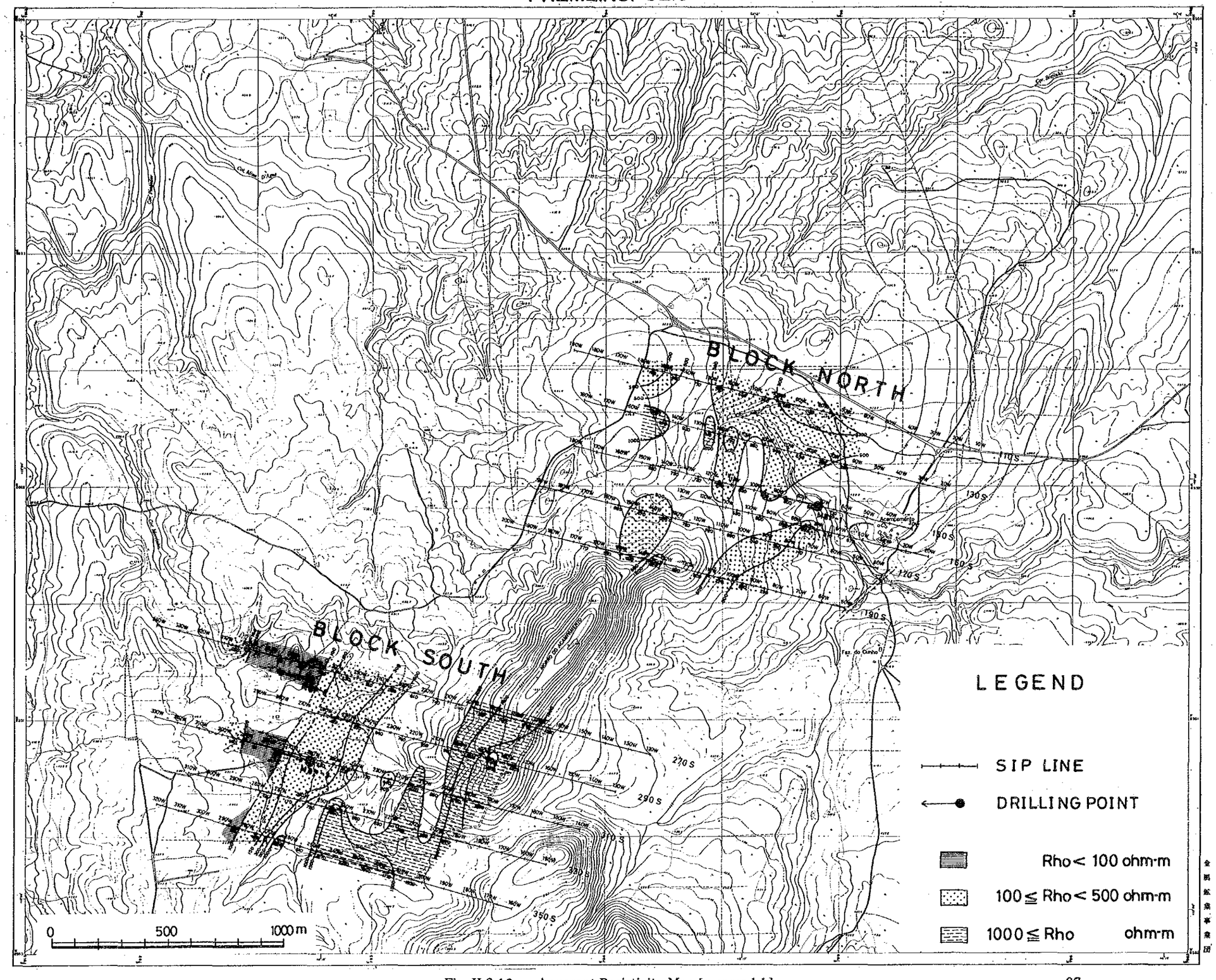

Fig. II-3-12 Apparent Resistivity Map [n-spread 1]

PALMEIRÓPOLIS

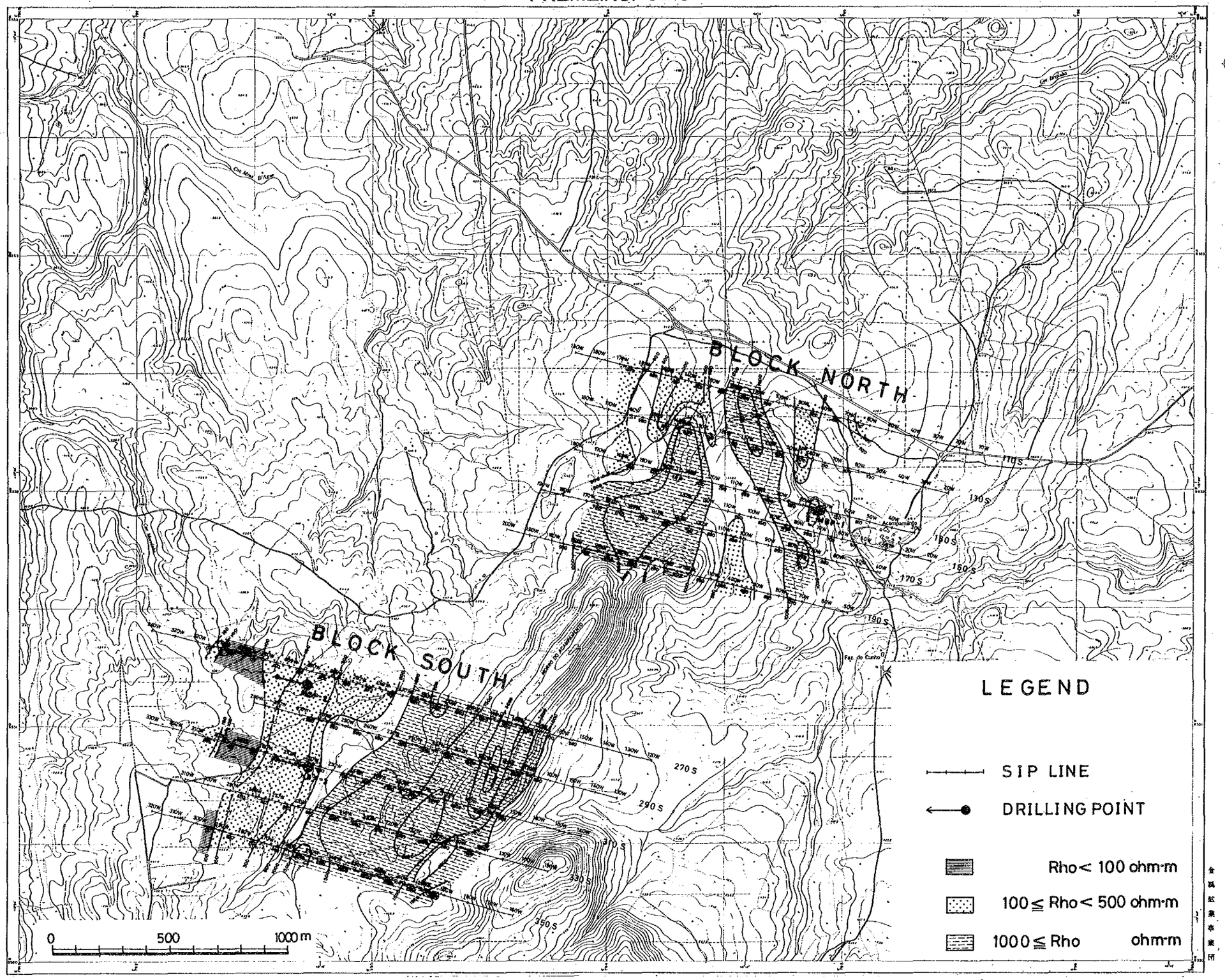

Fig. II-3-13 Apparent Resistivity Map [n-spread 3]

PALMEIRÓPOLIS

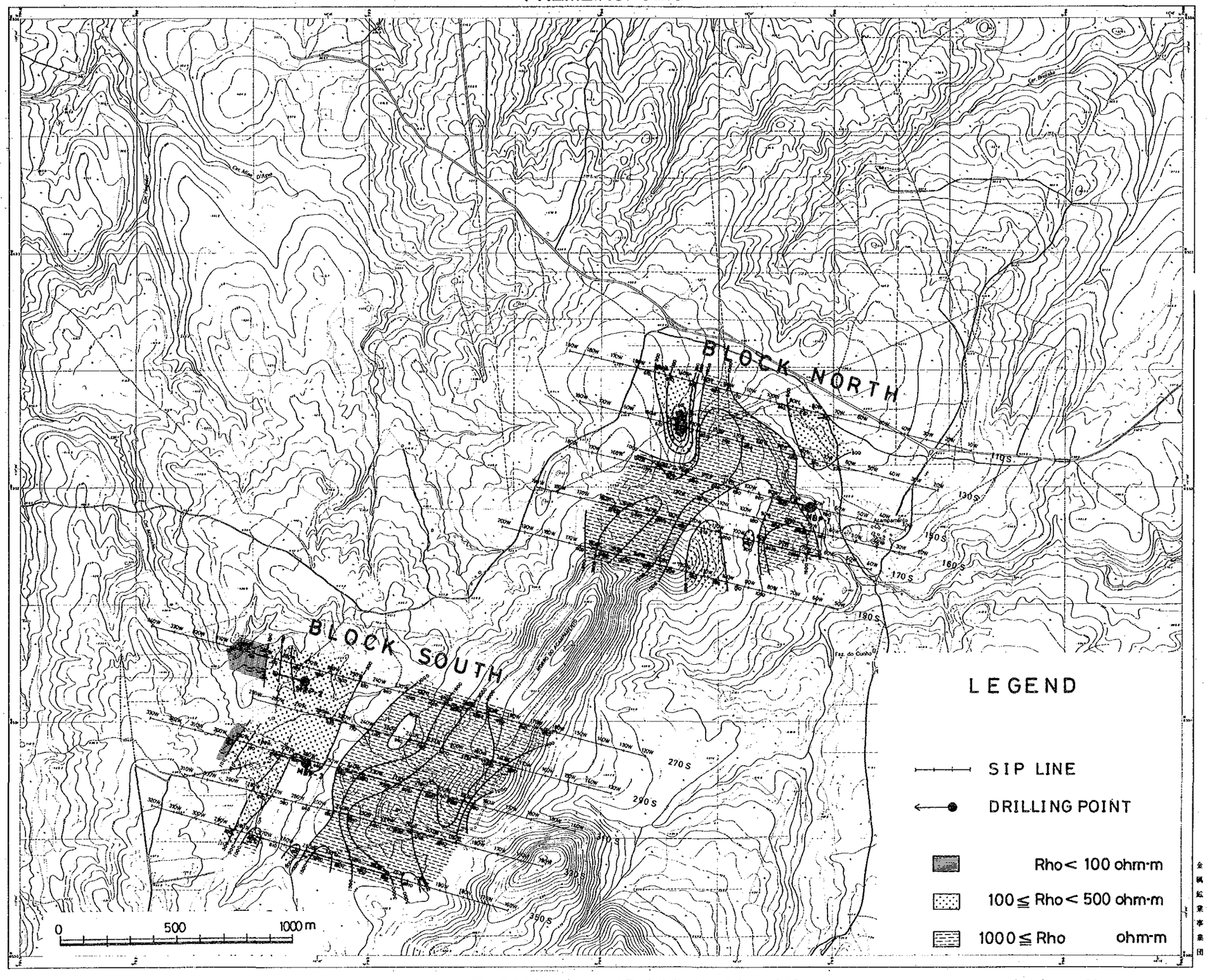

Fig. II-3-14 Apparent Resistivity Map [n-spread 5]

PALMEIRÓPOLIS

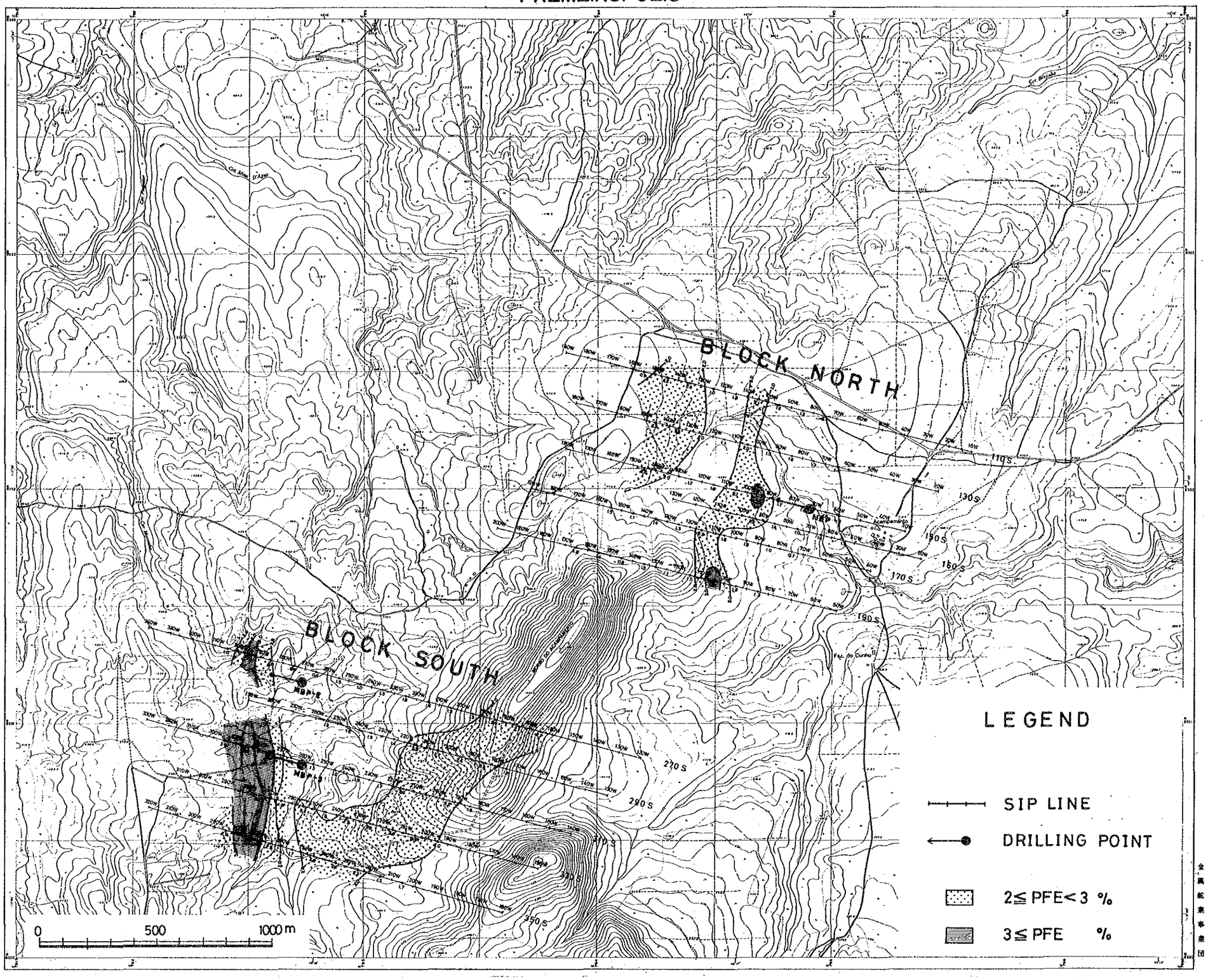

Fig. II-3-15 Frequency Effect Map [n-spread 1]

PALMEIRÓPOLIS

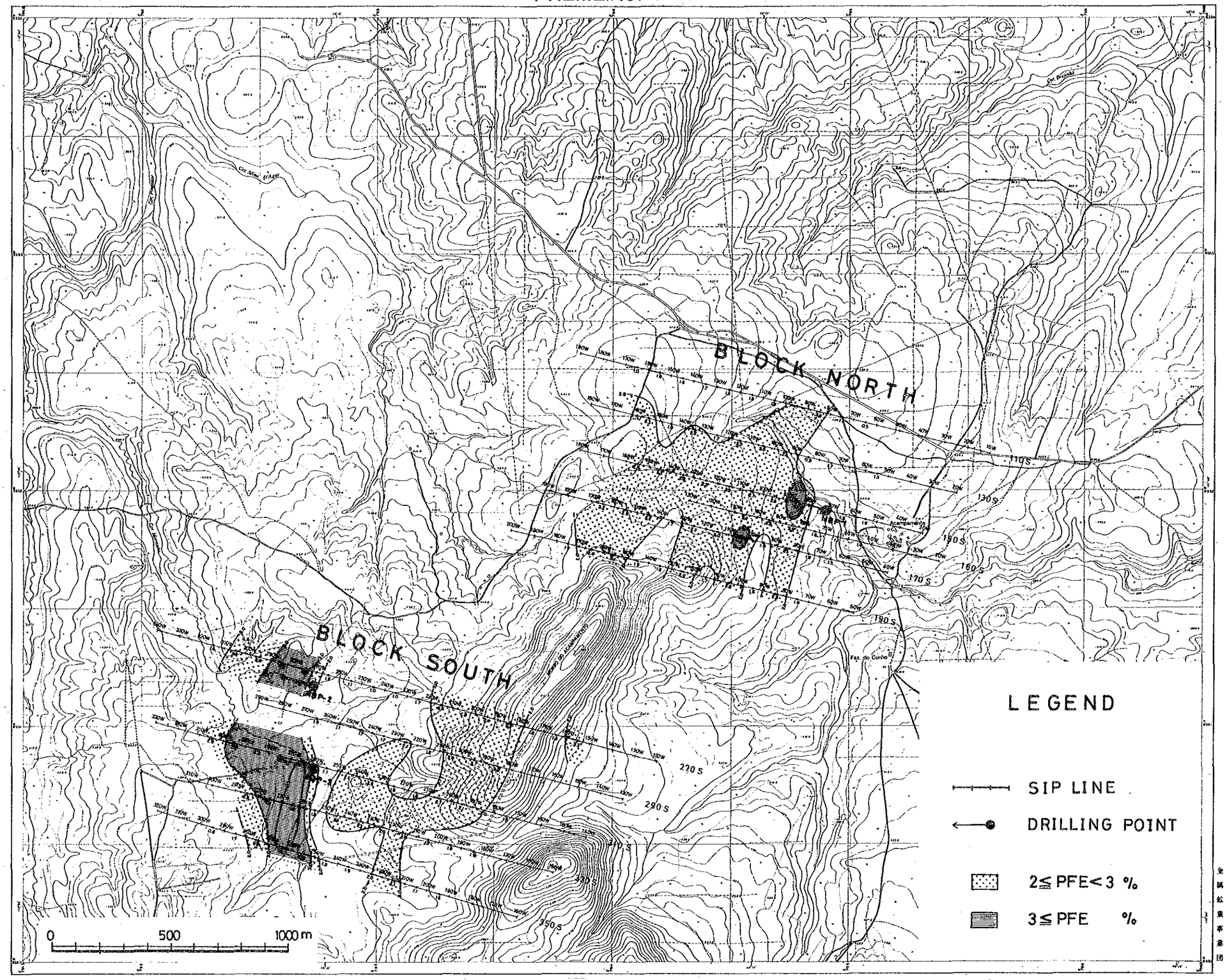

Fig. II-3-16 Frequency Effect Map [n-spread 3]

PALMEIROPOLIS

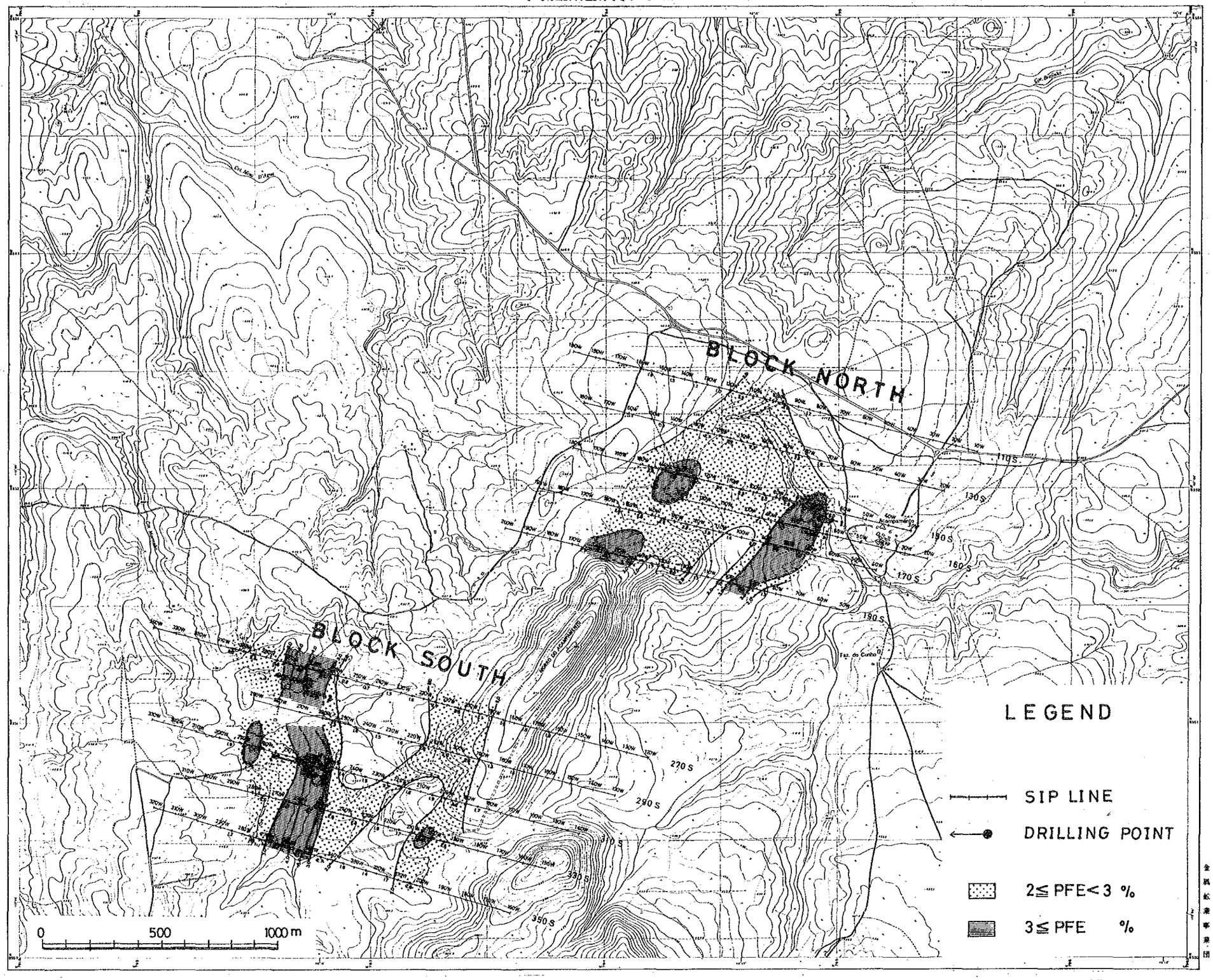

Fig. II-3-17 Frequency Effect Map [n-spread 5]

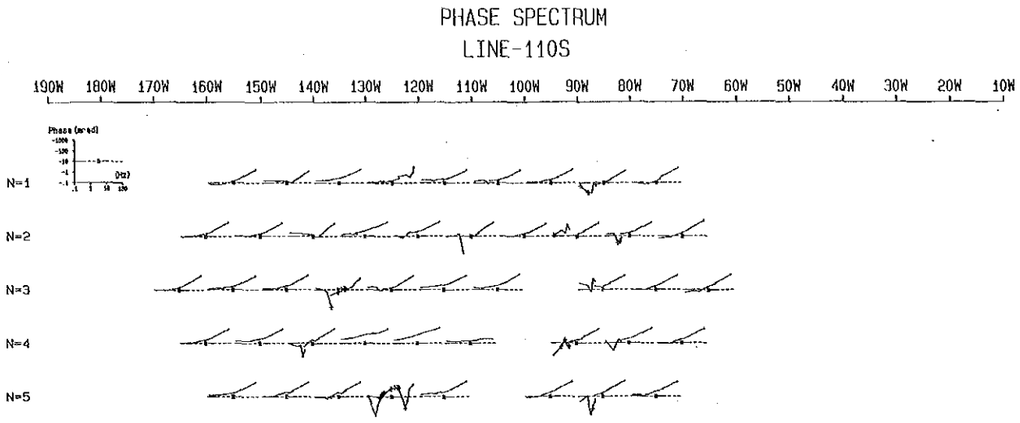

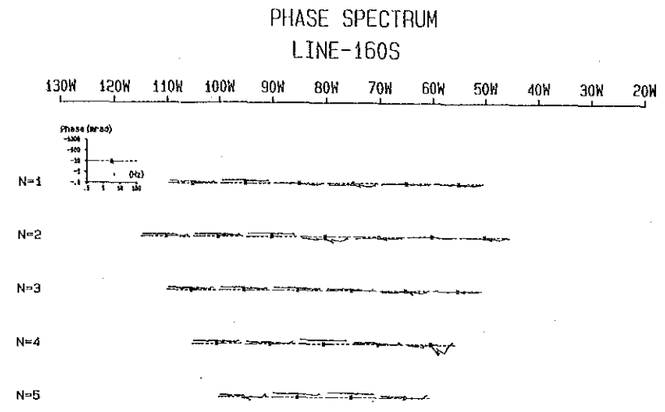

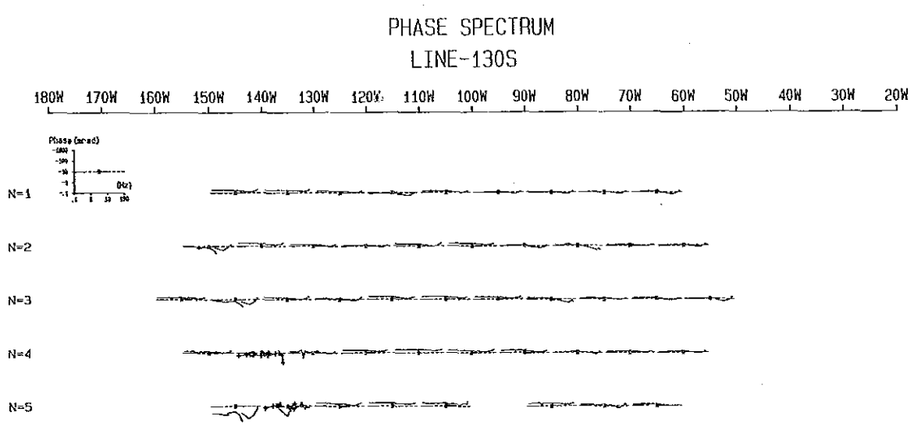

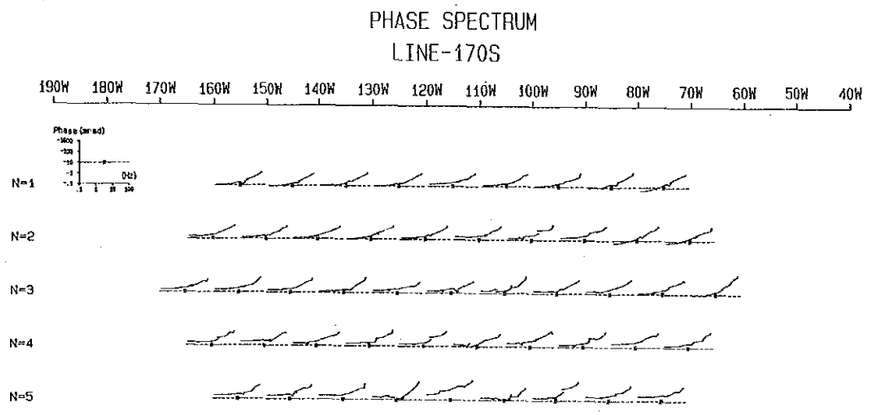

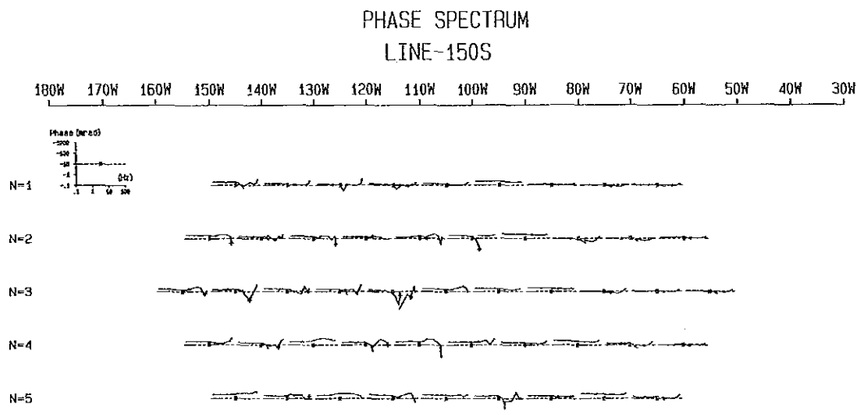

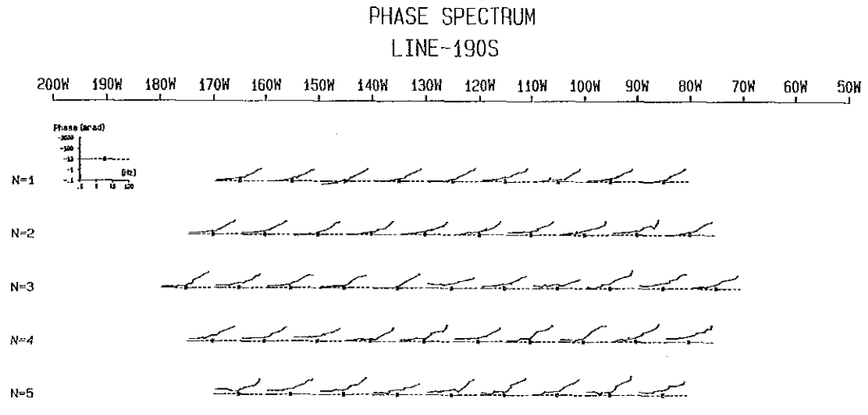

Fig. II-3-18 Phase Spectrum Diagram (Block North)

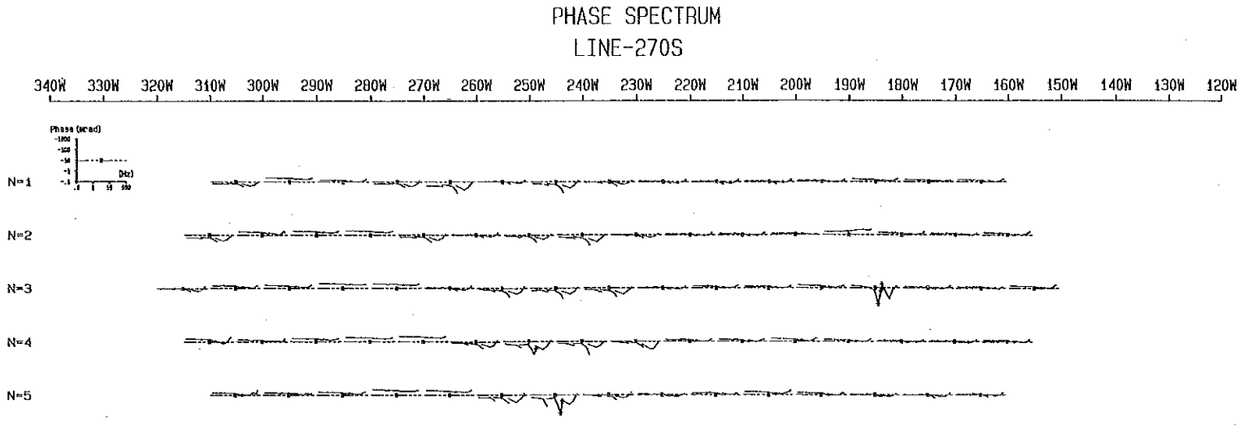

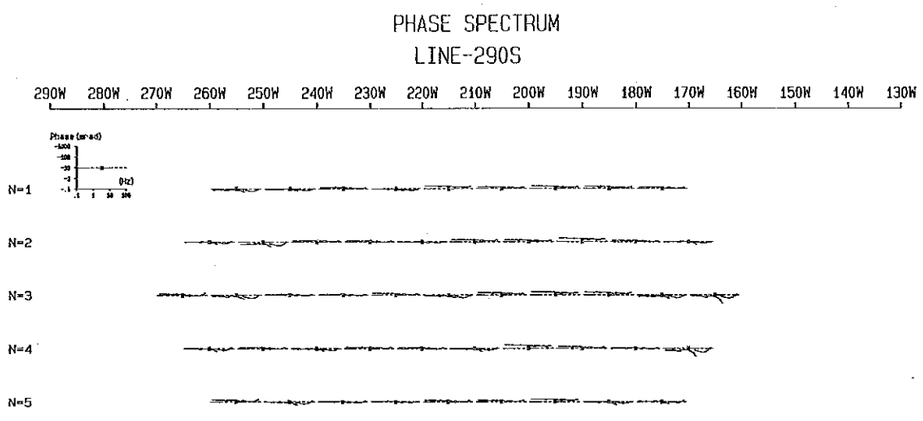

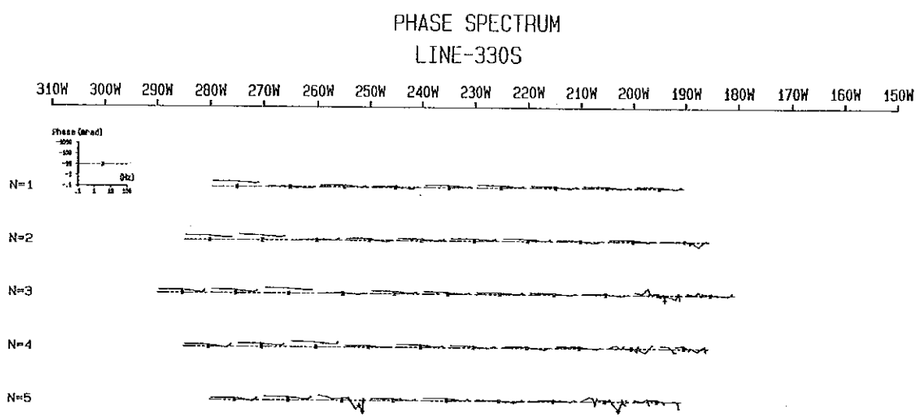

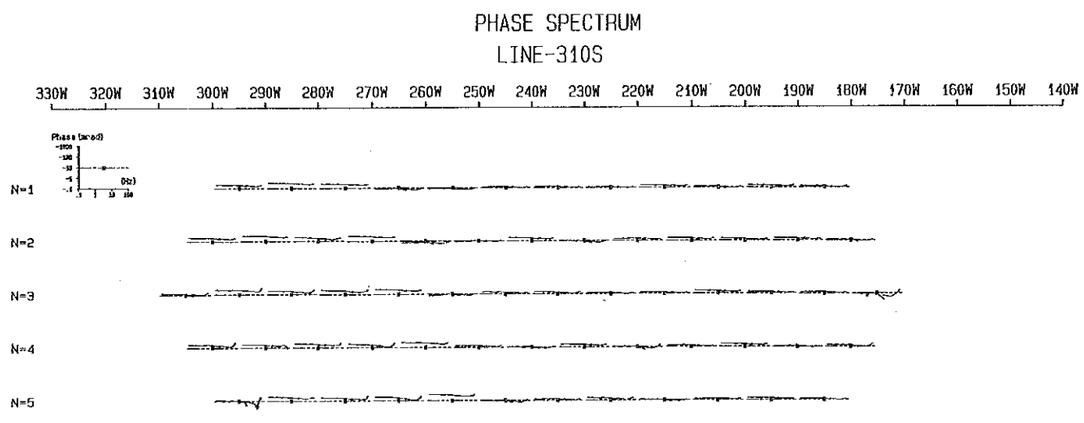

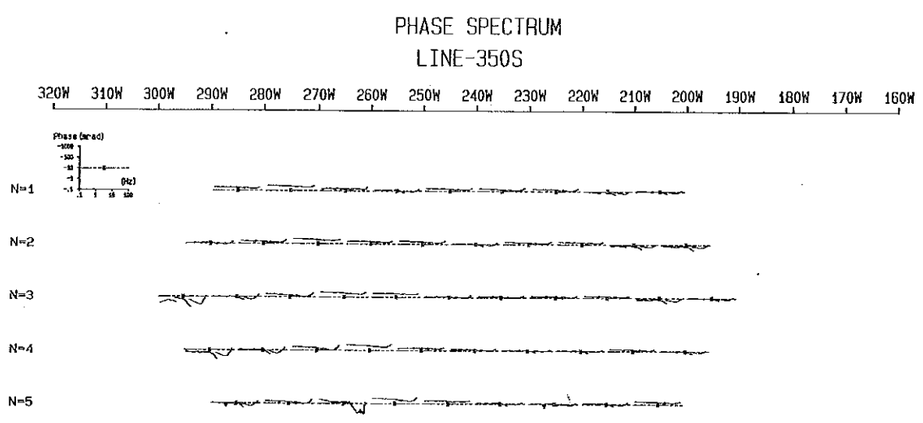

Fig. II-3-19 Phase Spectrum Diagram (Block South)

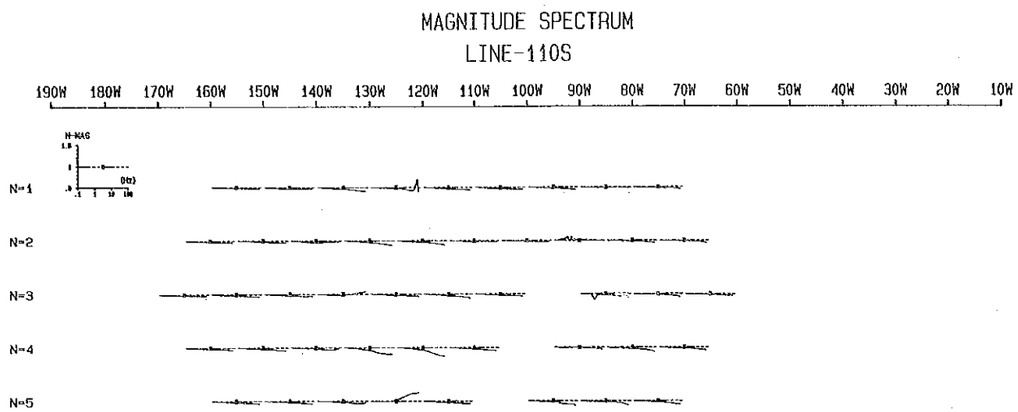

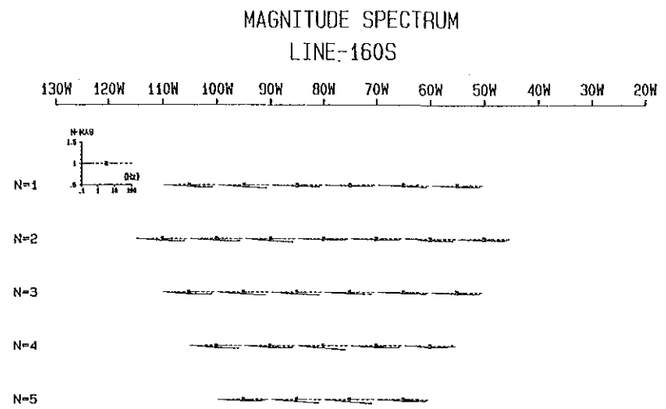

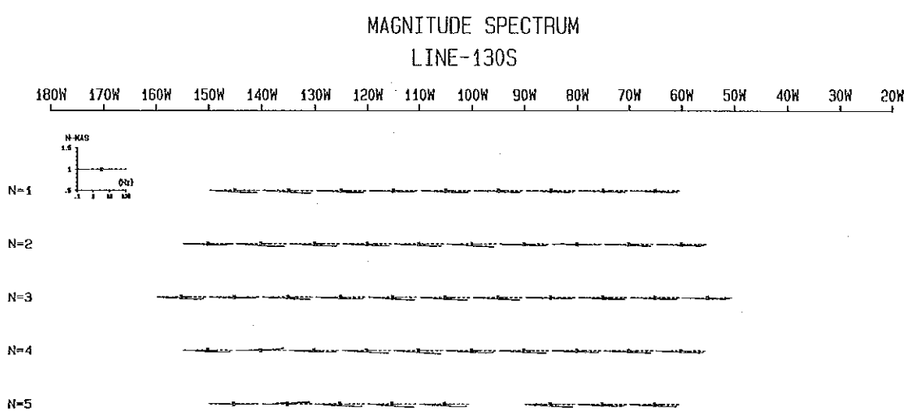

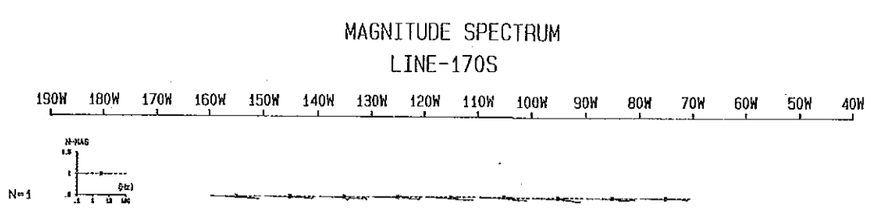

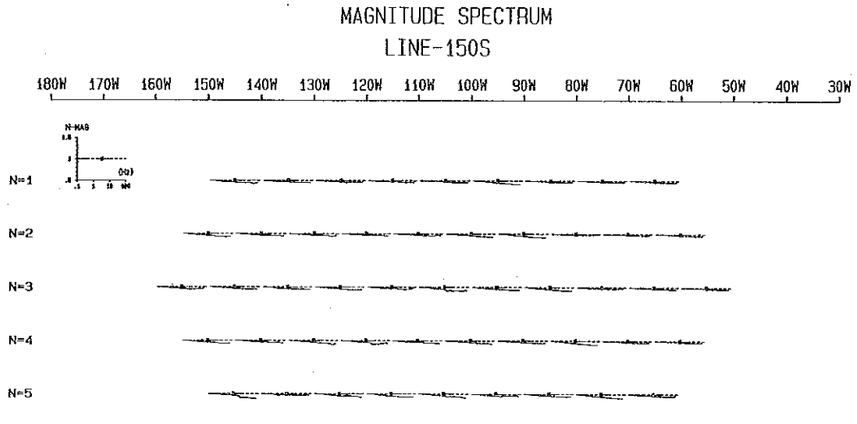

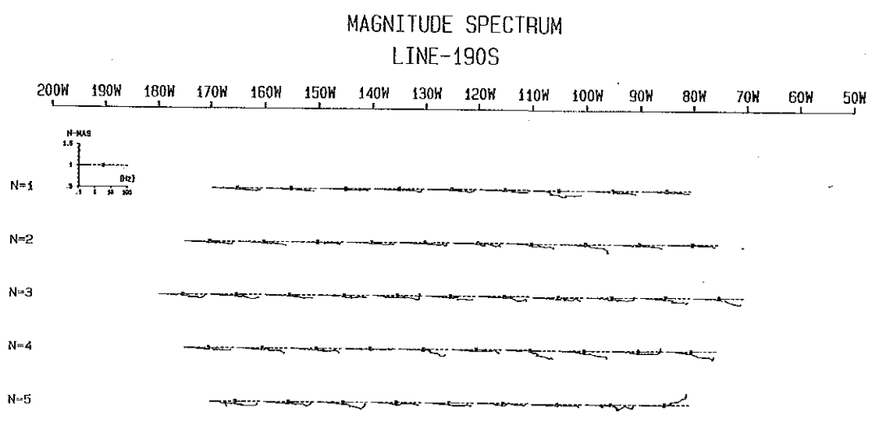

Fig. II-3-20 Magnitude Sectrum Diagram (Block North)

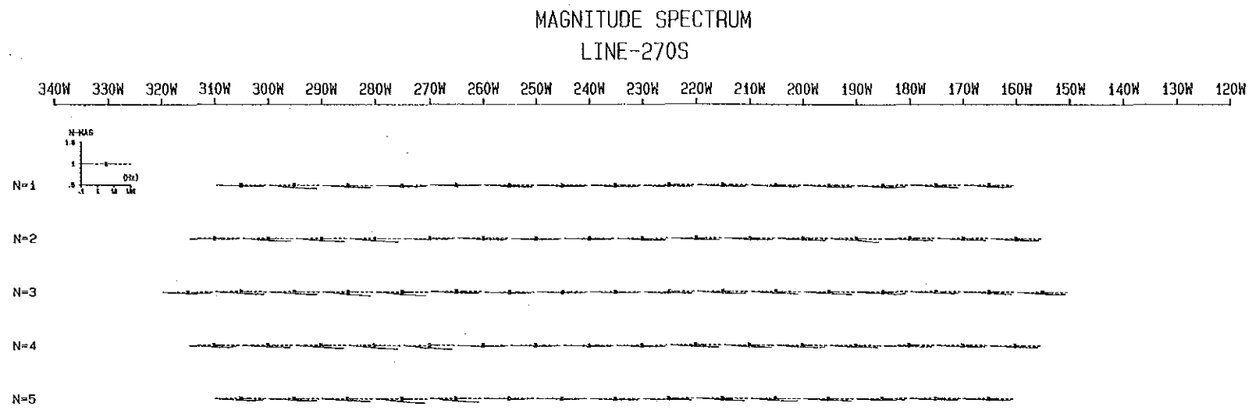

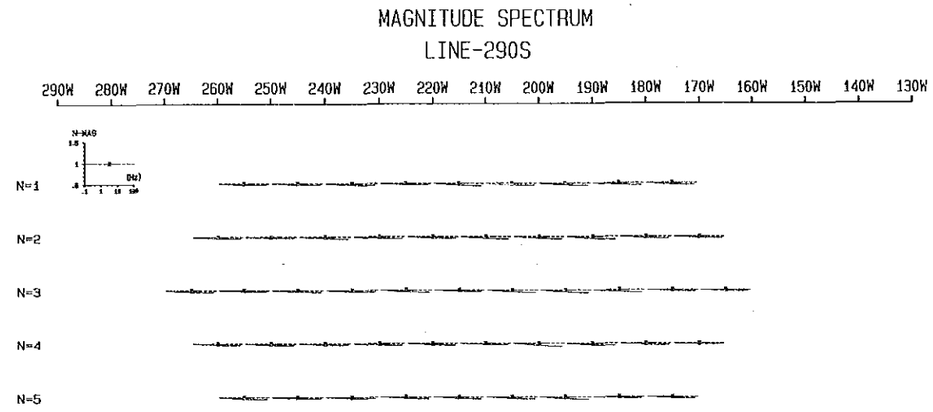

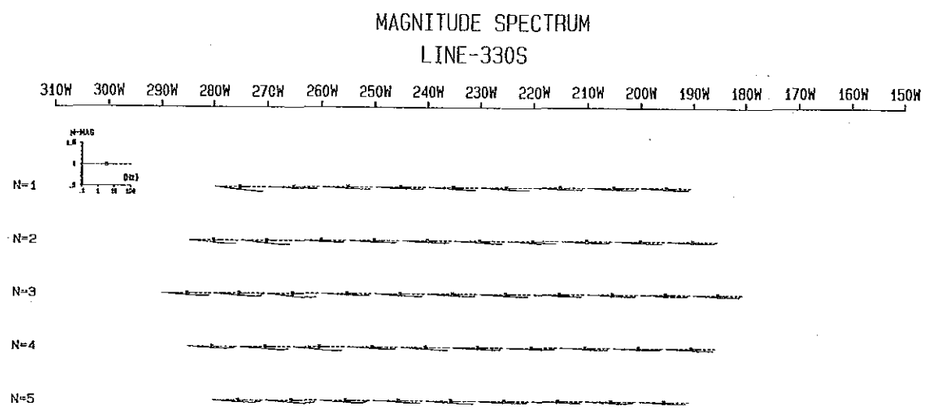

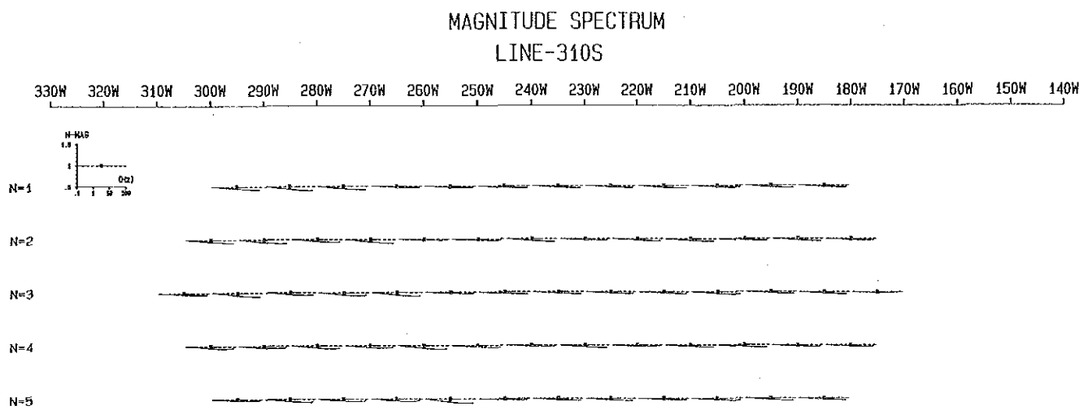

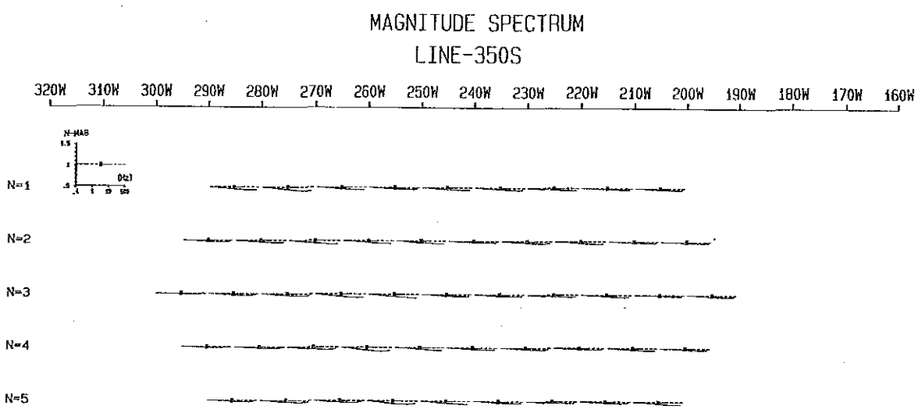

Fig. II-3-21 Magnitude Sectrum Diagram (Block South)

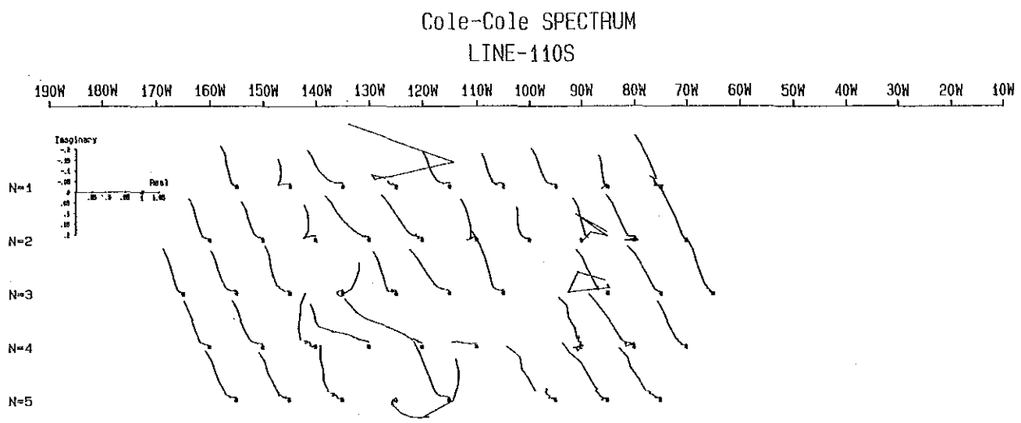

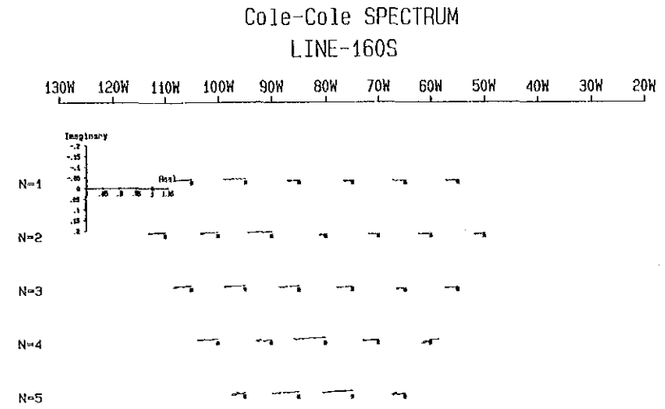

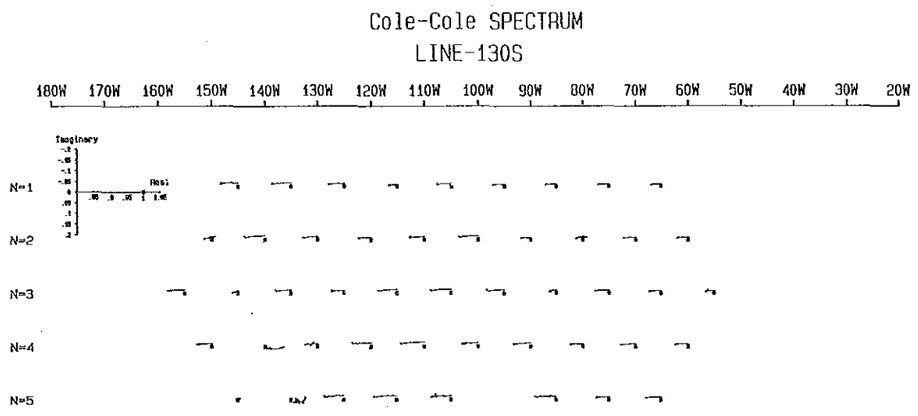

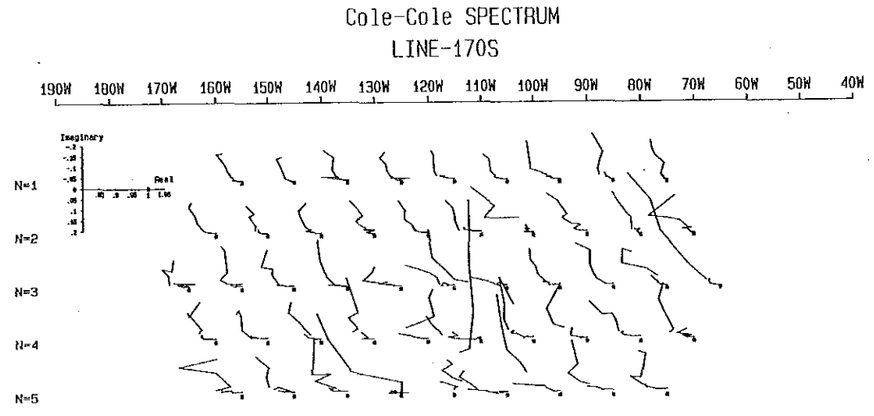

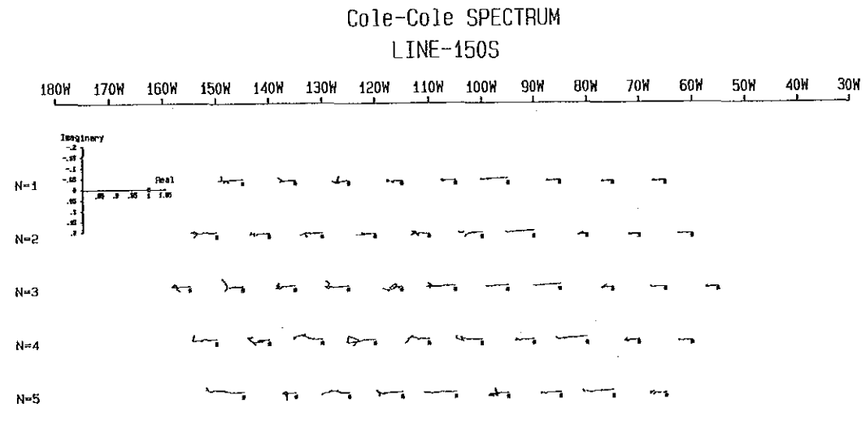

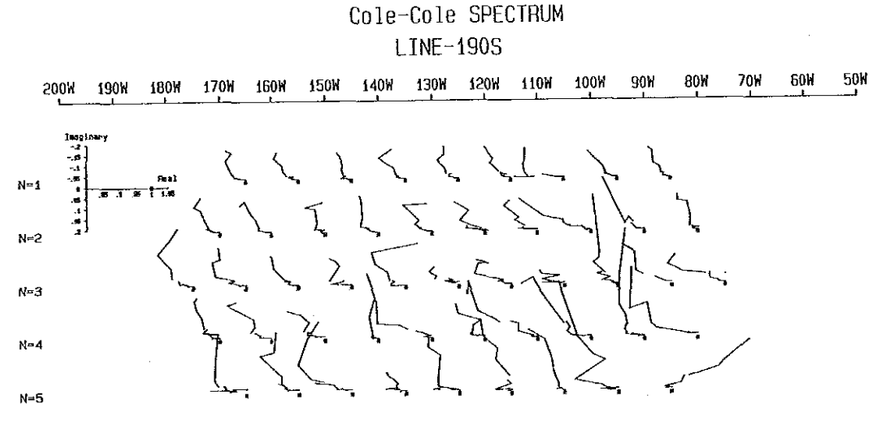

Fig. II-3-22 Cole-Cole Diagram (Block North)

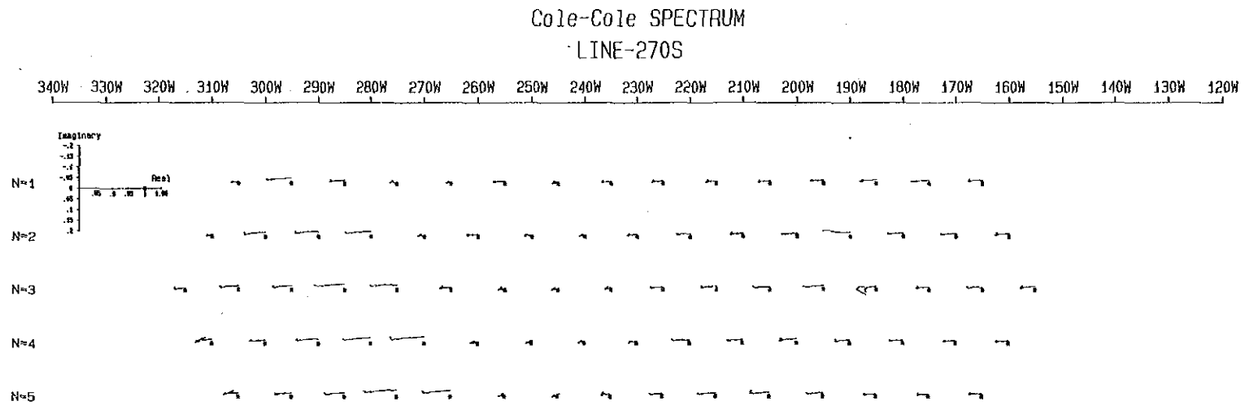

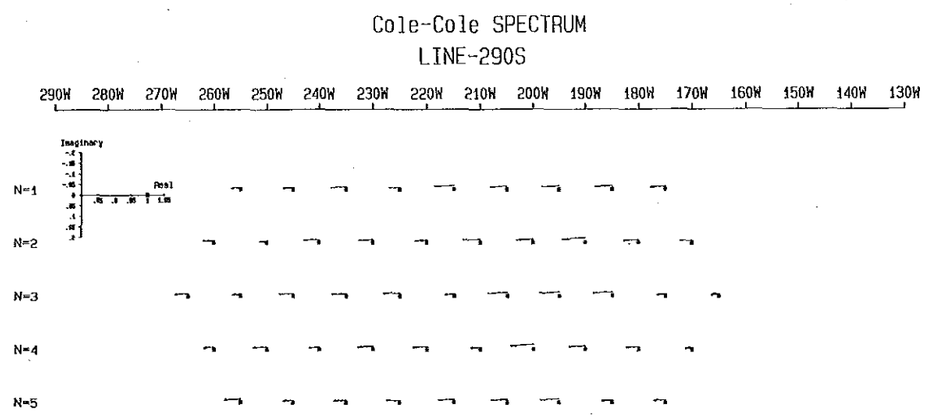

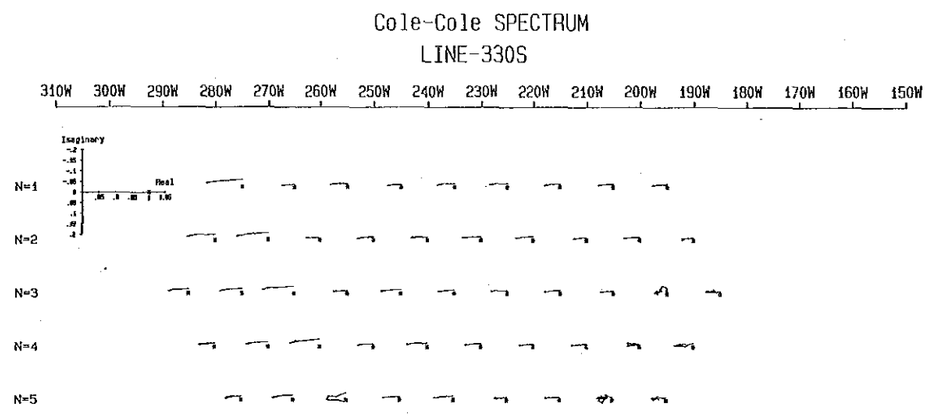

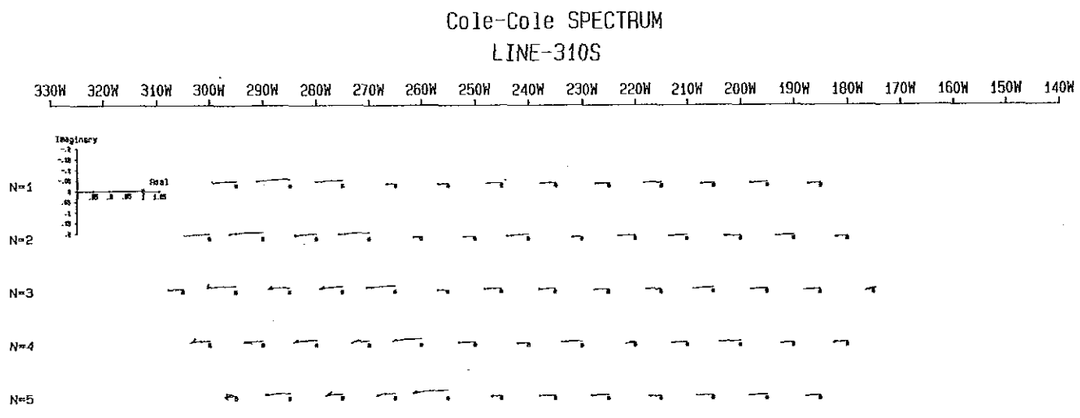

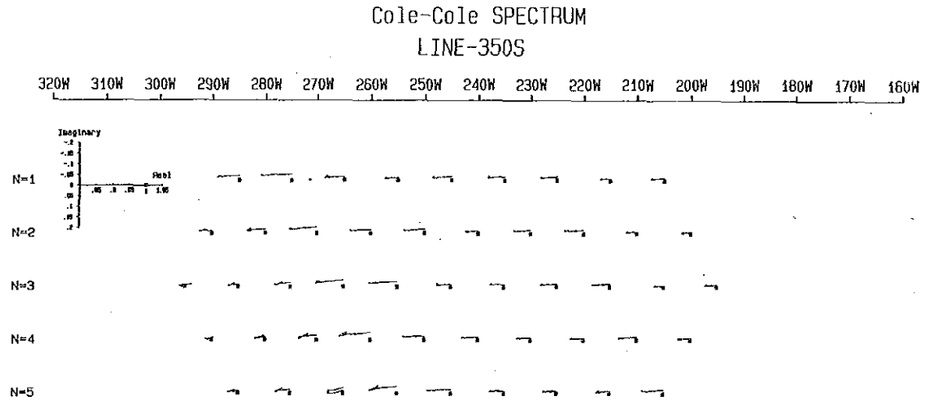

Fig. II-3-23 Cole-Cole Diagram (Block South)

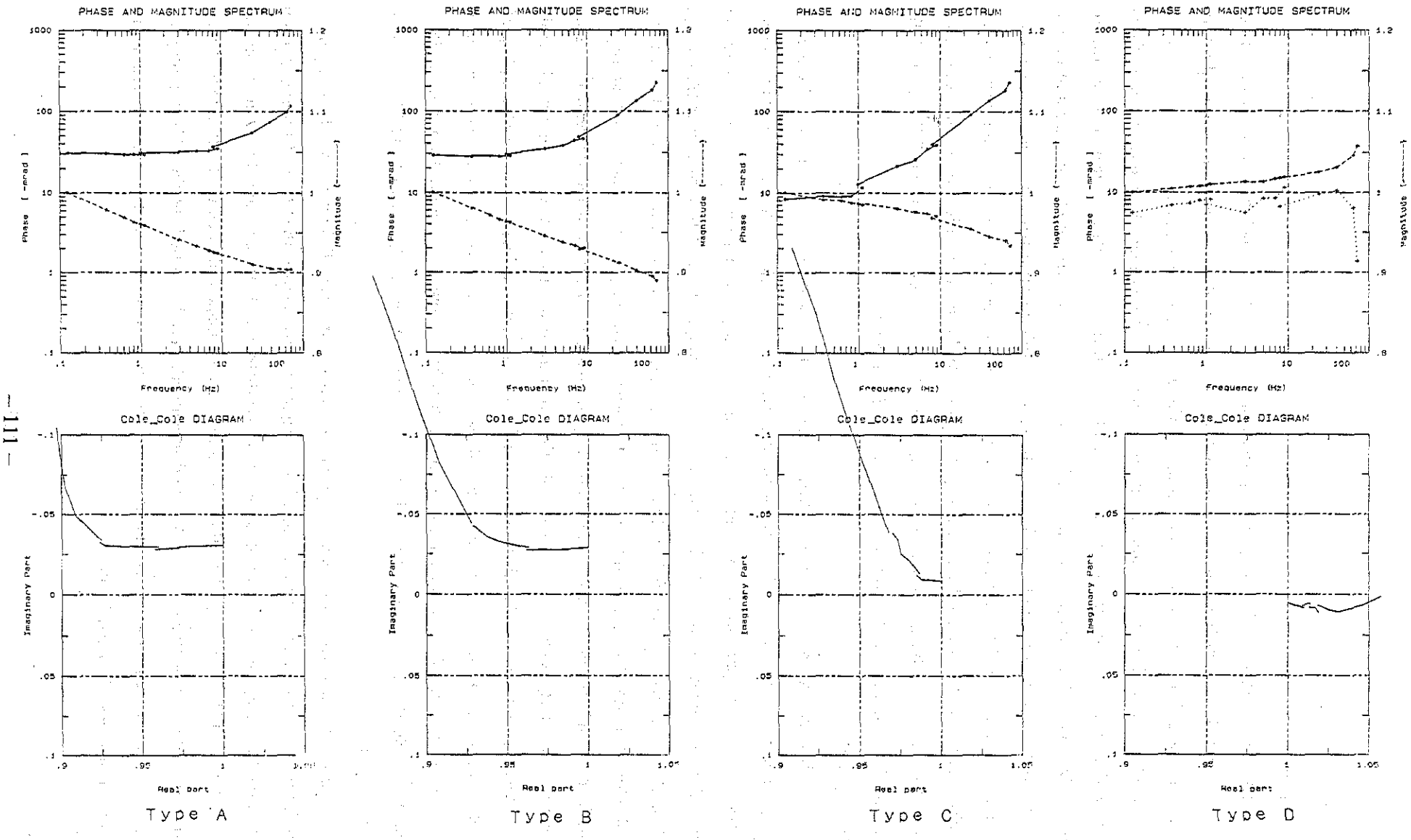

Fig. II-3-24 Spectrum of Typically Data

below.

(1) Type A

The characteristics of this spectral pattern are, 1) a peak of phase-difference is found between low and medium frequency ranges, 2) phase-difference decrease those value toward higher frequency, and 3) the strong IP effect is found at the whole frequency range.

And on the Cole-Cole diagram, a pattern of increase of imaginary part and decrease of real part with the increase of frequency can be found. This decrease of real part suggests to be due to mineralization and/or conductive body, which may correspond to sulfide minerals and/or graphite. And the negative coupling effect can be seen on this spectral pattern, which is caused by strong contrast of resistivities and may reflect the contact between graphite and surrounding rocks. Therefore, this spectral pattern may be caused by both of graphite and pyrite concentration. This spectral pattern is found at the deeper part than n=2 between stations 270W and 300W of Line 270S, and in the IP anomalous zone of the Block South.

2) Type B

In this spectral pattern, there is little variation of phase-difference at the low frequency range, but phase-differences decrease with increase of frequencies at higher frequency range. Little variation of phase-differences at lower frequency suggests that this type may correspond to highly conductive body, which eliminates the EM-coupling effect toward higher frequency. Then this type may reflect sulfide dissemination, which seems not to be compact, because on Cole-Cole diagram, decrease of imaginary part at lower frequency is not remarkable than that of the Type A and imaginary part increases abruptly at higher frequencies. While, decrease of magnitude at lower frequencies is not remarkable than that at higher frequencies. Therefore, it is said that this type reflects sulfide minerals at lower frequencies but is affected by the EM-coupling effect at higher frequencies. However, spectral pattern after the EM-decoupling shows a similar pattern as the Type A. This spectral pattern are distributed toward the south from Line 130S of the Block North, and is widely found in the high apparent resistivity zone of the Block South.

(3) Type C

This spectral pattern shows a monotonous increase of phase-differences on the raw phase-difference spectrum and the variation of the imaginary part is larger than that of the real part on the Cole-Cole diagram. However, decrease of phase-difference between 1 and 11 Hz are remarkable after the EM-decoupling. And there is no decrease of magnitude due to the IP effect. Therefore, this type, being treated as background in general, may be caused by the EM-coupling, and may reflect "barren rock". This spectral type are found at the distribution area of weathering schist near Lines 110S and 130S.

(4) Type D

This spectral pattern is caused by negative coupling, which is found at large variation of resistivities, that is, near fault-fractured zone, graphite and/or massive sulfide ore deposits. At the Block North, there are a lot of type D in Line 110S, so fault-fractured zones with NNE-SSW trend are infered on Line 110S. And at the Block South, this type are found at several locations in the western IP anomalous zone and those seem to reflect resistivity difference between graphite and surrounding schist.

3–1–4 Model Simulation

The 2-D model simulation using the finite element method (FEM) was carried out in order to understand the deeper distribution of IP anomalous sources in both blocks, and the southward extension of the contact of graphite and sulfide minerals in the Block South. Survey lines objective for 2-D model simulation are Lines 150S and 170S in the Block North, and Lines 370S, 310S and 350S in the Block South.

Code numbers in 2-D model corresponding to resistivity and phase are assigned taking into consideration of geological conditions and the results of drilling survey and physical property measurement. Resistivities and phases of each code were changed by trial and error until good approximation of calculated values to observed values can be met.

The results are described as follows:

(1) Line 160S

An IP anomaly is found between 70W and 100W. Code #8 (800 ohm-m, –40 mrad) was set for an IP anomaly with P.F.E. of 2.0 to 3.0% caused by pyrite dissemination, and #11 (3,000 ohm-m, –40 mrad) for a deep IP anomaly of more than 3.0% between stations 70W and 90W. And code #1 (800 ohm-m, –10 mrad), #3 (400 ohm-m, –10 mrad) and #7 (3,000 ohm-m, –10 mrad) are set as background.

The result is given in Fig. II–3–25. Apparent resistivity distribution is thought to be almost same as that of the observed. And a deeper anomaly at depth of –250 mGL seems to show similar pattern as that of the observed, but local anomaly of phase-difference of –20 mrad at the depth of n=2 and 3 at station 90W can not be presented.

2) Line 170S

IP indications of P.F.E. of more than 2.0% are widely distributed. Code #3 (3,000 ohm-m, –20 mrad) and #5 (3,000 ohm-m, –40 mrad) were set for IP anomalies of P.F.E. of 2.0 to 3.0%, caused by sulfide (pyrite) dissemination zone. Model with large phase were assumed to explain several IP anomalies of P.F.E. of more than 3.0% at stations 110W and

100W, and between stations 70W and 90W, but no good result was obtained. Code #1 (800 ohm-m, −15 mrad), #4 (400 ohm-m, −15 mrad) and #2 (200 ohm-m, −15 mrad) were set at the east of station 110W and at the shallower part at the west of station 120W.

The final result is shown in Fig. II−3−26. Calculated pattern of apparent resistivity distribution shows a good approximation with that of the observed, but the contrast found in the observed P.F.E. pseudosection can not be presented.

3) Line 270S

IP indications of more than 2.0% are found at the east of station 220W and between stations 260W and 310W, but as the former indication is thought to be due to shallower dissemination, model setting for this indication was not done. While the latter indication seems to be due to shallower and deeper sources, so three codes were assigned. Code #4 (50 ohm-m, −10 mrad) and #5 (50 ohm-m, −40 mrad) for shallower sources were set at west-dipping from station 250W and at east-dipping from station 290W, and code # (600 ohm-m, −40 mrad) for deeper source was set at east-dipping from the depth of −75 mGL at station 290W. And code #1 (300 ohm-m, −10 mrad), #2 (600 ohm-m, −10 mrad), #3 (3,000 ohm-m, −15 mrad) and #8 (600 ohm-m, −25 mrad) were set for background.

Model and final result are shown in Fig. II−3−27. IP indications detected between stations 270W and 300W are almost reappeared in the calculated pseudosection.

4) Line 310S

Three IP anomalous sources may exist in this line. Within three sources, as an IP anomalous source between stations 190W and 220W seems to be an extension from Line 270S, no model setting for this source was made. For other two anomalous sources, code #2 (20 ohm-m, −25 mrad) and #5 (500 ohm-m, −40 mrad) were set. And in order to explain medium and high resistivity layers, code #3 (500 ohm-m, −10 mrad) and #4 (3,000 ohm-m, −15 mrad) were set respectively. While, code #1 (300 ohm-m, −10 mrad) for background was set.

Model section is shown in Fig. II−3−28. Calculated result shows good approximation with the observed, but the values of IP indication is a little higher than those of the observed. A little high value will be decreased if code #4 and #5 increase those thickness a little.

5) Line 350S

P.F.E. values of more than 2.0% are widely distributed at the west of station 200W, and form a bload IP anomalous zone, which may reflect two IP anomalous sources; one is distributed between stations 230W and 240W, and other one shows east-dipping from the surface of station 280W. Code #5 (5,000 ohm-m, −30 mrad) and #4 (2,500 ohm-m, −15 mrad) were set for the former source, and code #6 (40 ohm-m, −40 mrad) and #7 (1,000 ohm-m, −40 mrad) for the

latter source. And code #2 (40 ohm-m, −15 mrad) and #3 (1,000 ohm-m, −15 mrad) were set for background.

Model and final result are shown in Fig. II−3−29. The calculated section shows good approximation with the observed.

LINE-160S JOB:063 (0.125Hz)

MESH SELECT OPTION : 2 69X14

CODE NUMBER	1	2	3	4	5	6	7	8	9	10
RESISTIVITY (Ohm-m)	800.0	250.0	400.0	3000.	800.0	400.0	3000.	800.0	800.0	3000.
PHASE (m-radians)	10.0	10.0	10.0	25.0	20.0	20.0	10.0	40.0	25.0	40.0

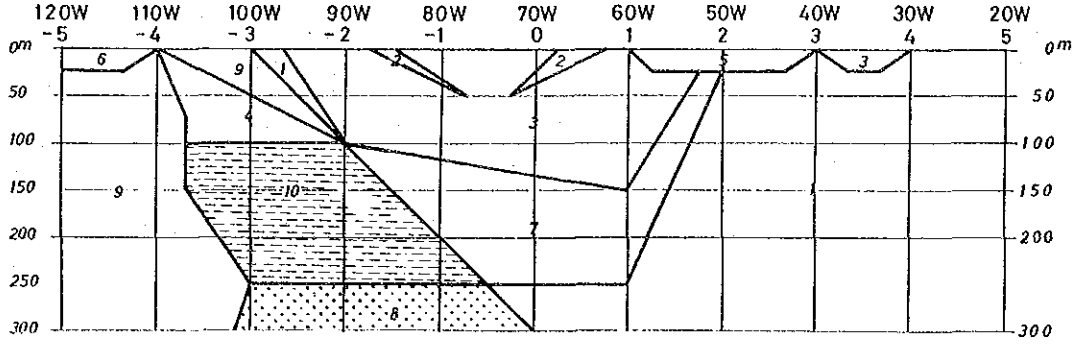

APPARENT RESISTIVITY (OHM-METERS)

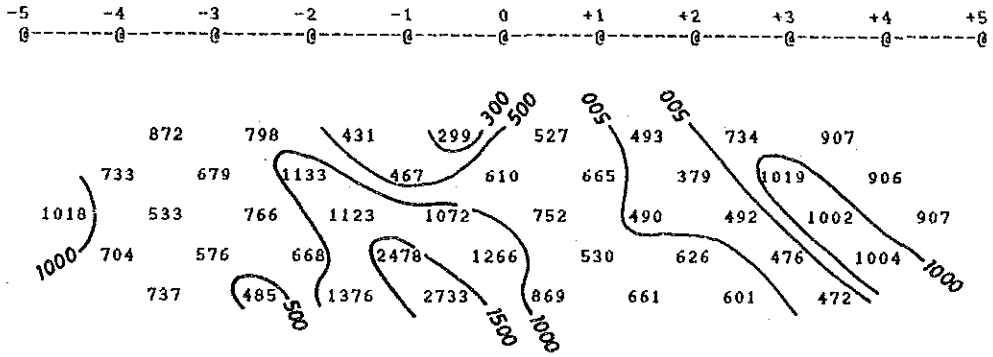

APPARENT PHASE

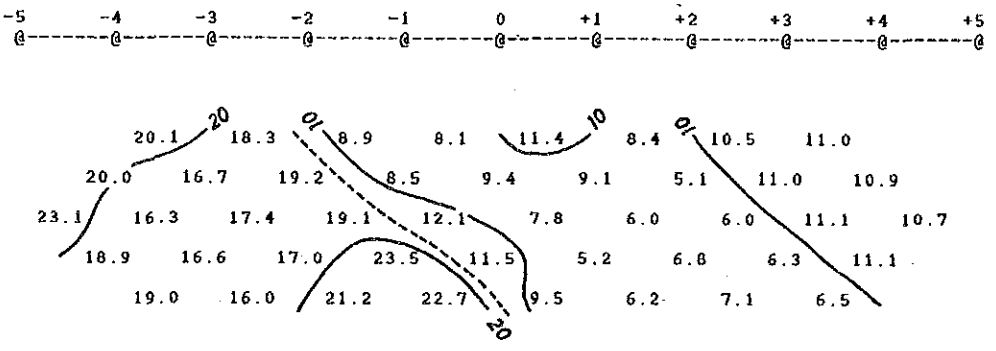

Fig. II-3-25 2-D Model Calculation (Line-160S)

LINE-170S JOB:033 (0.125 Hz)

MESH SELECT OPTION : 2 69X14

CODE NUMBER :	1	2	3	4	5	6	7	8	9
RESISTIVITY (Ohm-m) :	800.0	200.0	3000.	400.0	3000.	800.0	800.0	400.0	3000.
PHASE (m-radians) :	15.0	15.0	20.0	15.0	40.0	10.0	20.0	10.0	15.0

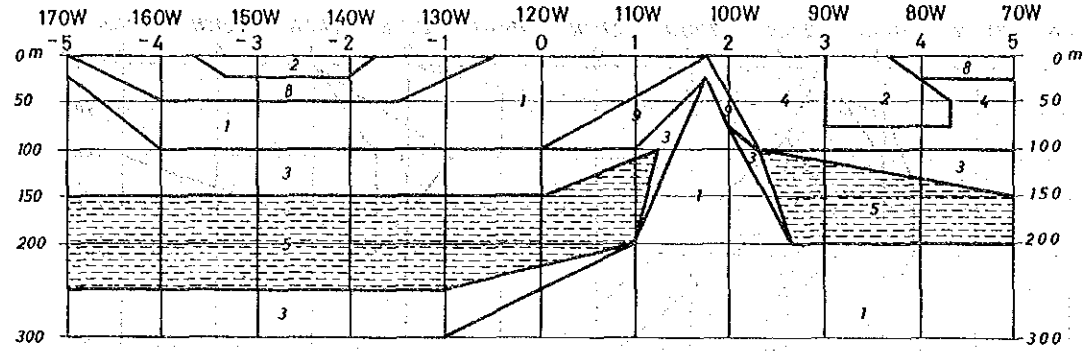

APPARENT RESISTIVITY (OHM-METERS)

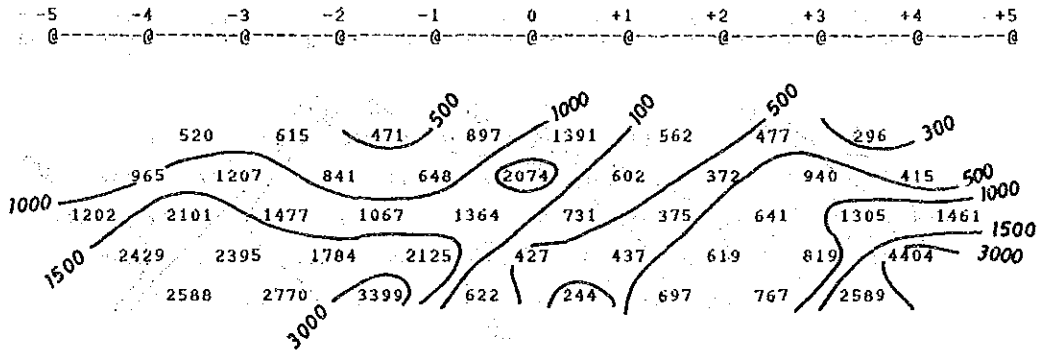

APPARENT PHASE

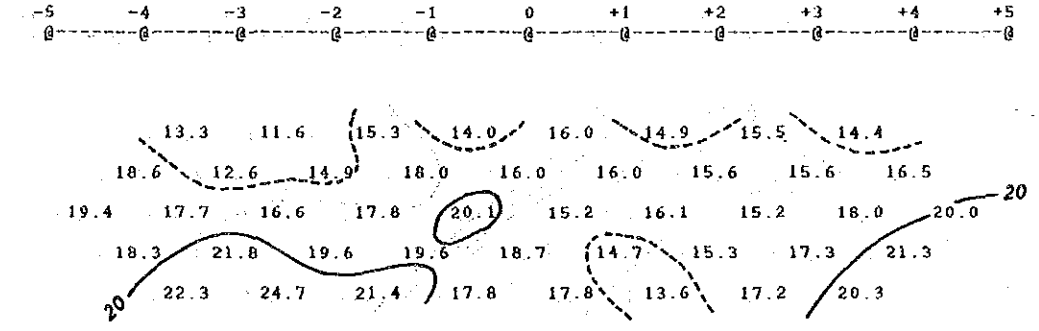

Fig. II-3-26 2-D Model Calculation (Line-170S)

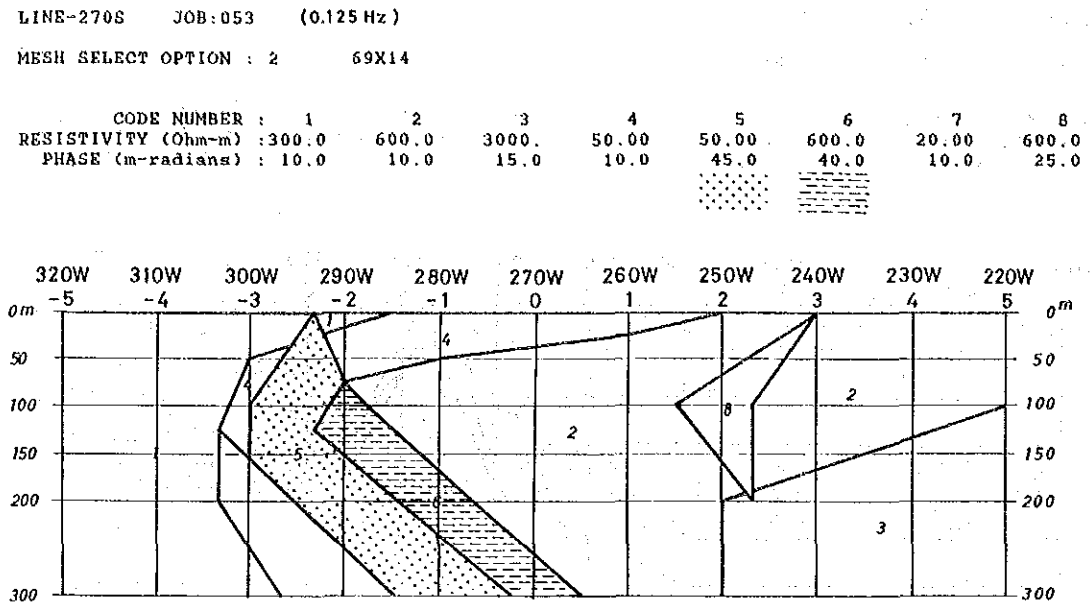

APPARENT RESISTIVITY (OHM-METERS)

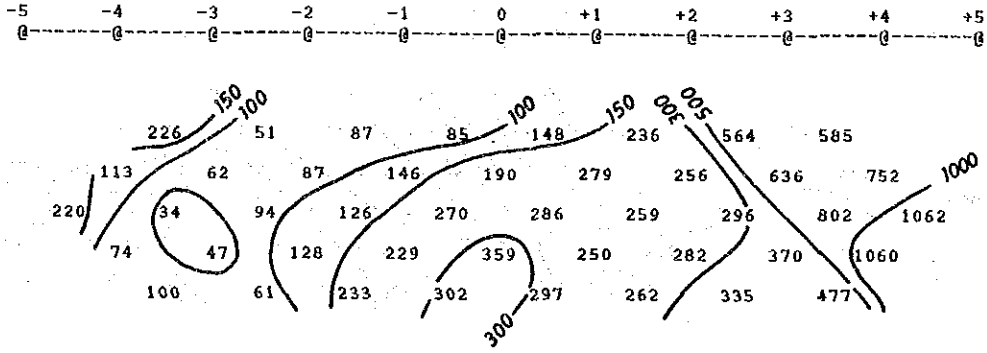

APPARENT PHASE

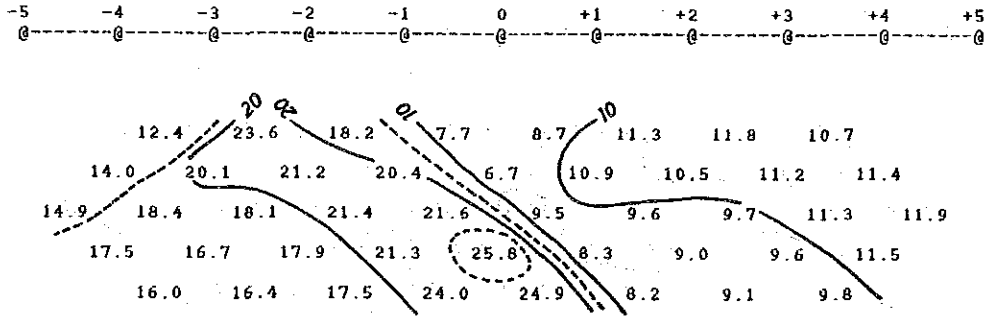

Fig. II-3-27 2-D Model Calculation (Line-270S)

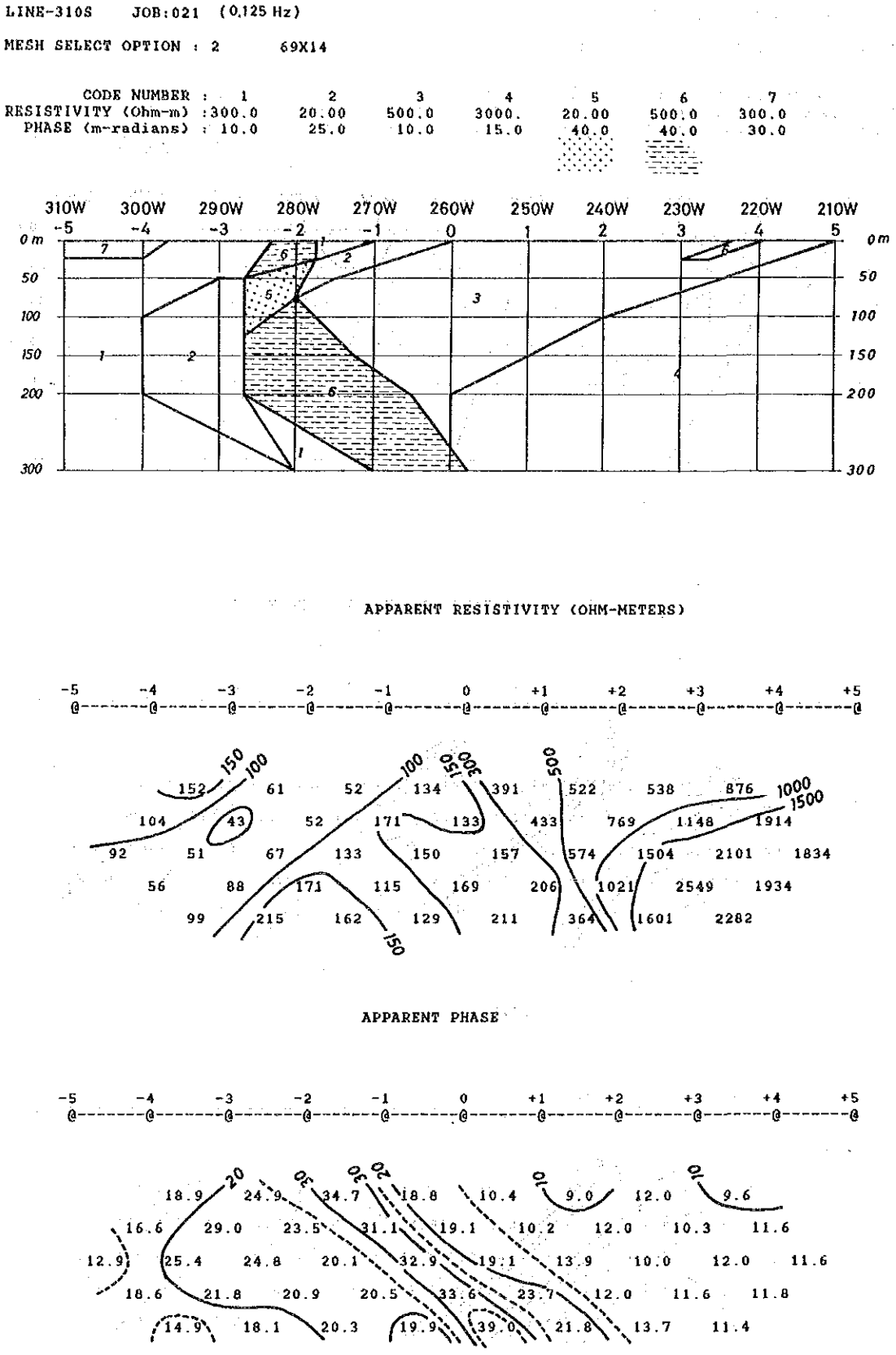

Fig. II-3-28 2-D Model Calculation (Line-310S)

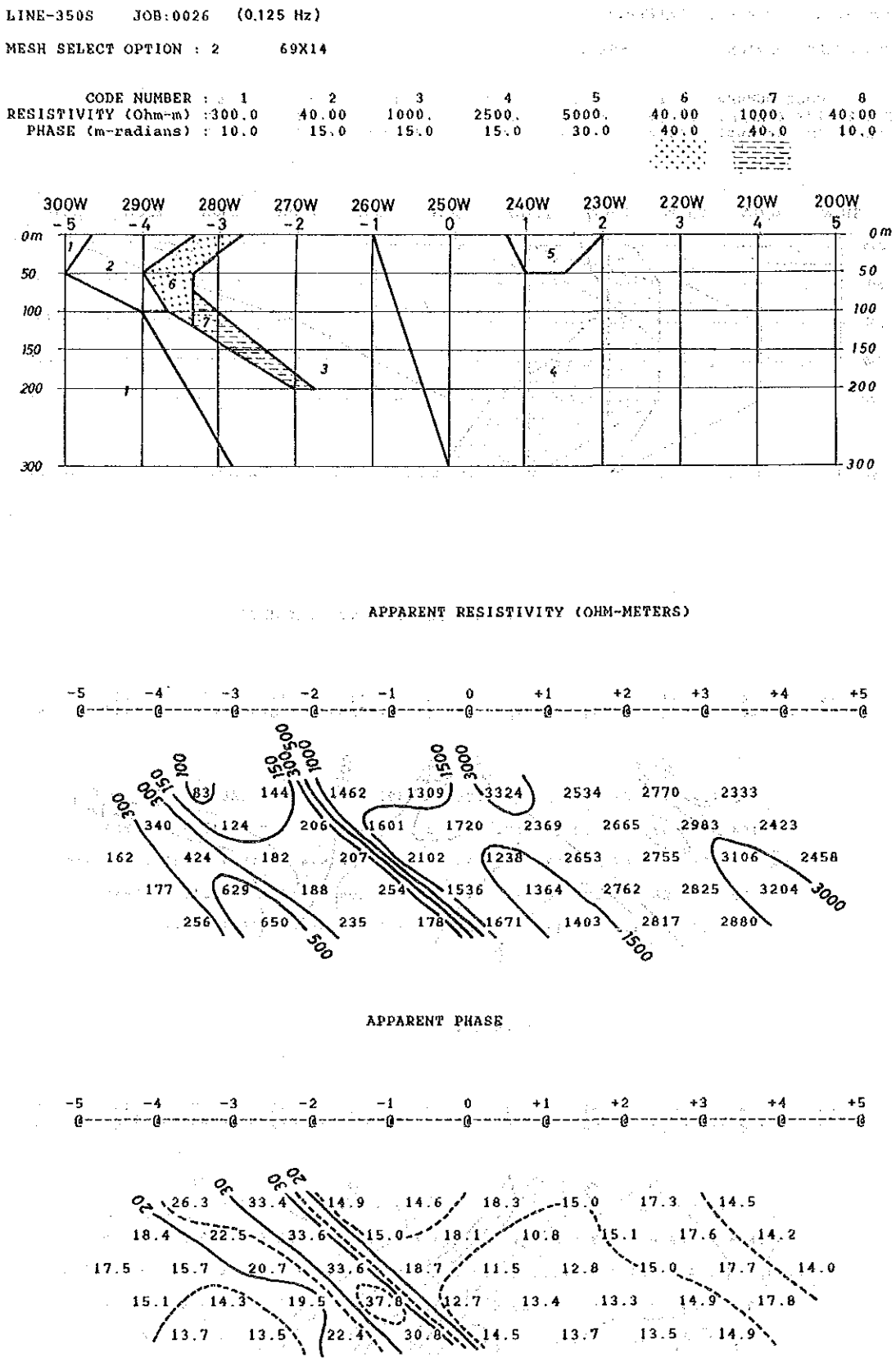

Fig. II-3 29 2-D Model Calculation (Line-350S)

3–2 Results of Drilling Survey

As can be seen in the geological columnar sections (1 : 200) of each hole, the names of rocks are difficult to determined in some parts because constituent minerals abruptly change at every interval of 50 cm, and therefore each mineral is shown by broken line (Fig. II–3–30) so as to be understood visually.

Although quantitative comparison of main constituent minerals, accessory minerals and ore minerals is possible among each mineral, the comparison is of no meaning as they belong to different categories.

3–2–1 Geology and Mineralization of Hole MBP–1

(1) Location

The hole was located along a tributary of Corrego do Mato about 300 m to the west-northwest of the CPRM camp, at a point E794.90 longitude and N8551.91 latitude.

(2) Surface Geology of the Surroundings

The hole was located along a tributary of Corrego do Mato about 300 m to the west-northed in 1987 and by the work of CPRM (1984) as follows.

Amphibolite of the Pip_3 formation is distributed at the place about 800 m to the east of the hole, conginuing from the C–1 ore body located to the north-northeast. Similar amphibolite is found about 300 m to the northwest of the hole. Both rock bodies show an overturned anticlinal structure toward the east, and the anticlinal axes extend in the direction of NNE–SSW and plunge southward.

The hole is located on the southeastern limb of the anticline on the northwest, and the area is widely underlain by mica-quartz schist of the Pip_4 formation which overlies amphibolite of the Pip_3 formation.

Actually, the exposure is very poor because of wide covering of laterite and Canga, limonitized laterite, and sand and gravel, and therefore the geology of the surroundings (Fig. II–3–31) was estimated based on the occurrence of a great number of floats. Hence the details of geologic structure can not be made clear.

(3) Geology of the Hole

0.00 ~ 1.60 m :

The section consists of brown soil, and subround gravel of quartzite are found at the lowest part.

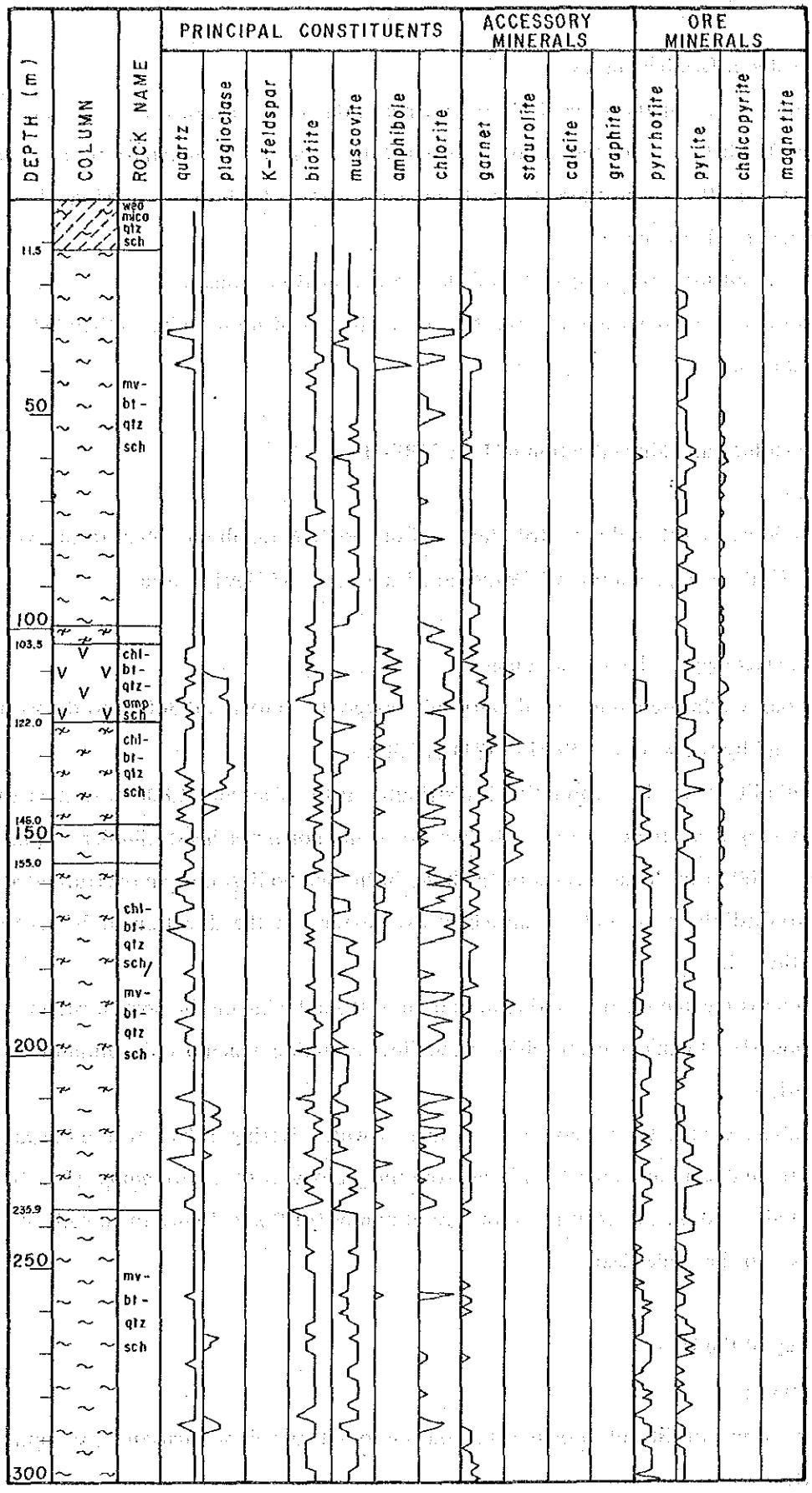

Fig. II-3-30 (1) Generalized Columnar Section of Core Logs (MBP-1)

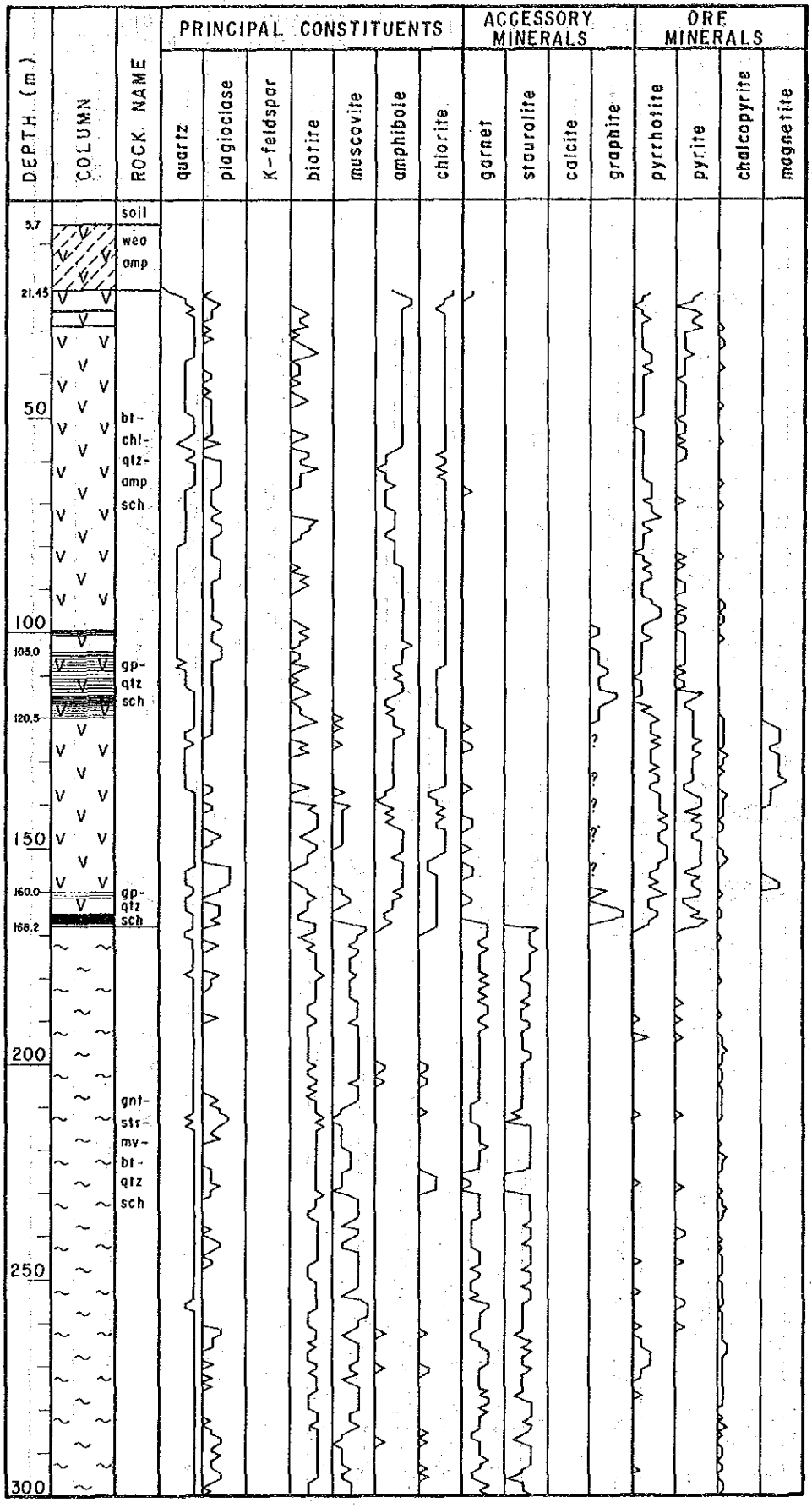

Fig. II-3-30 (2) Generalized Columnar Section of Core Logs (MBP-2)

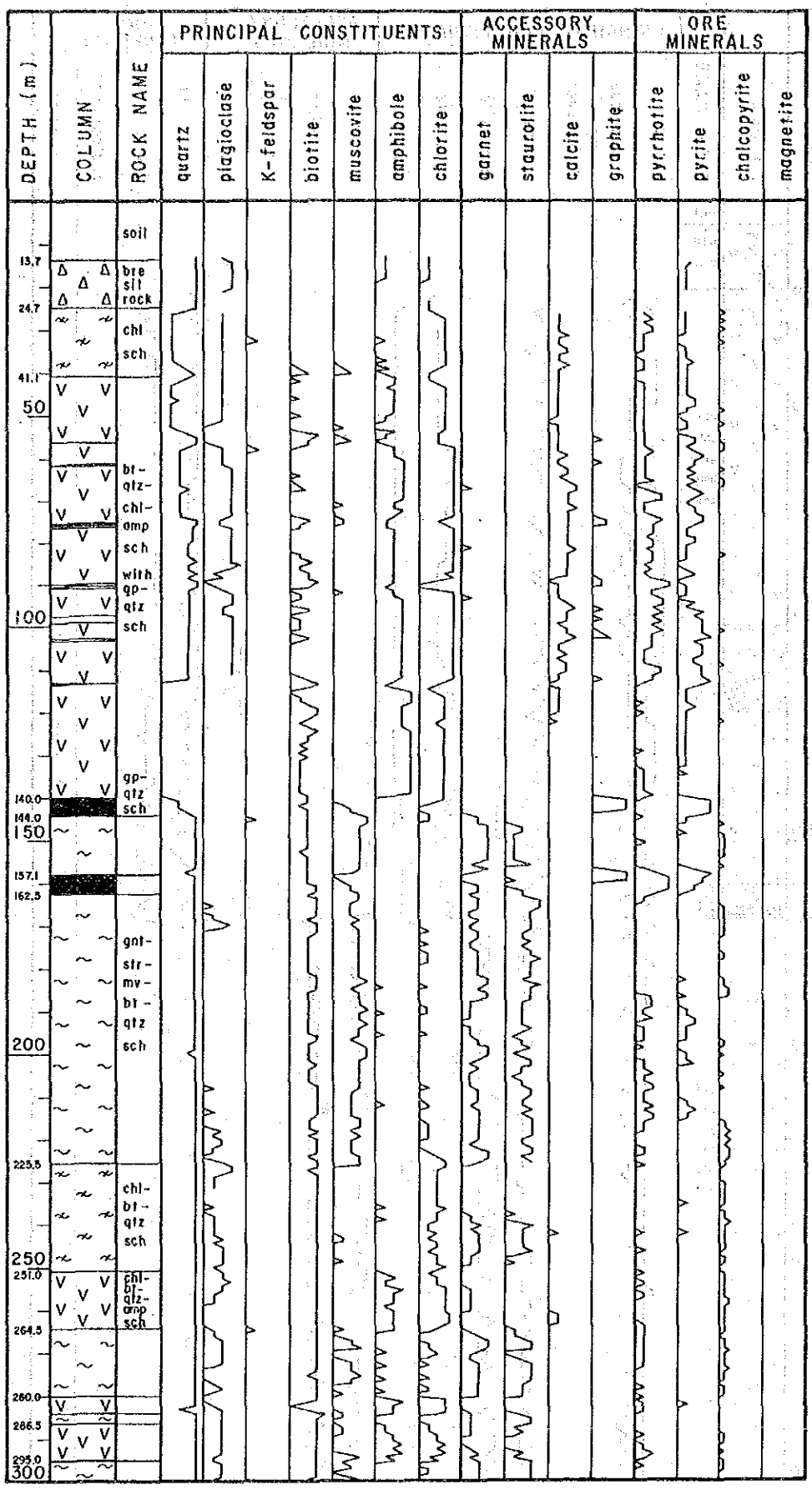

Fig. II-3-30 (3) Generalized Columnar Section of Core Logs (MBP-3)

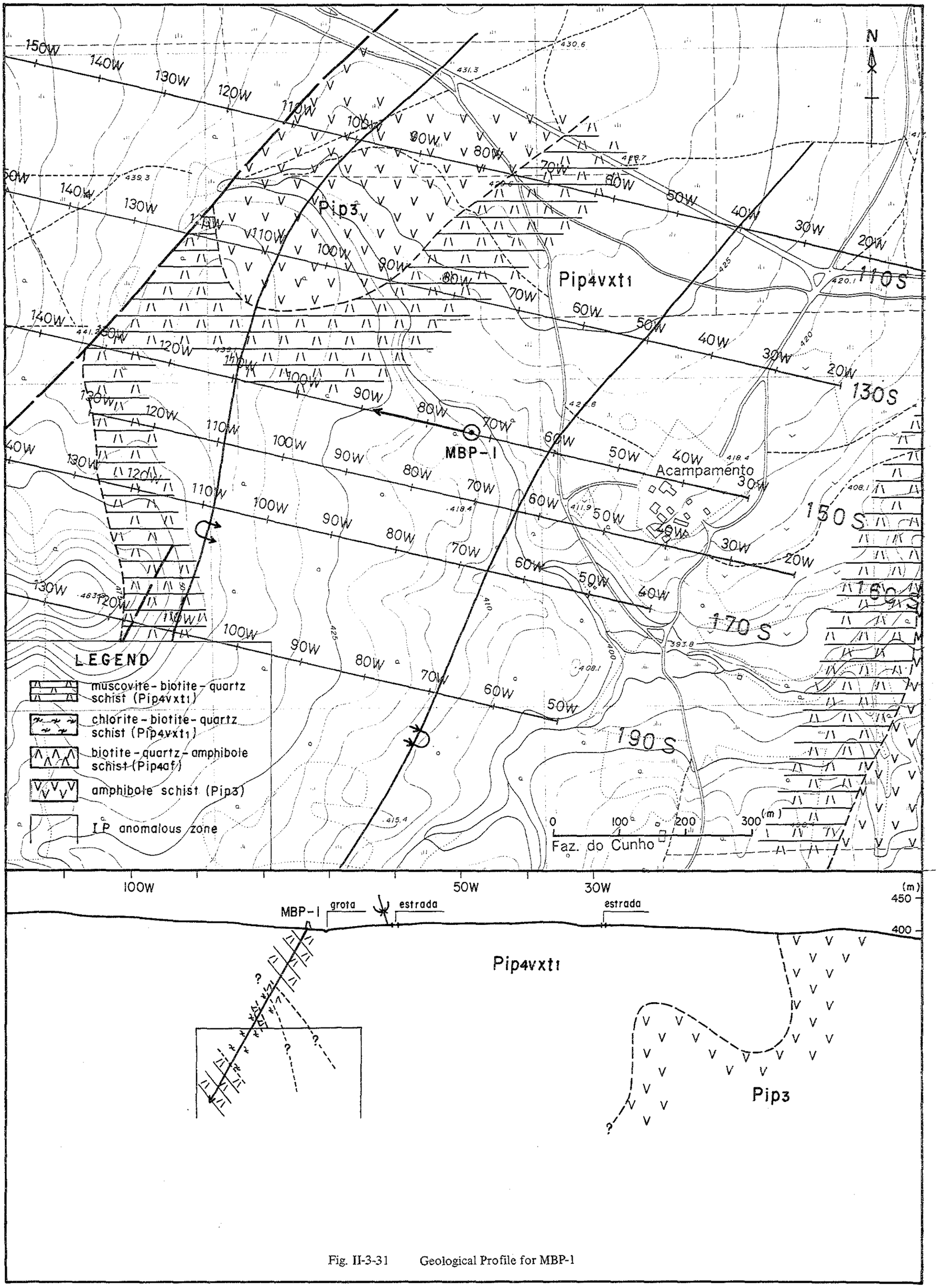

Fig. II-3-31 Geological Profile for MBP-1

1.60 ~ 11.50 m :

The rock consists of gray, highly weathered mica-quartz schist. Descrimination between biotite and muscovite in the rock is difficult because of weathering.

11.50 ~ 99.00 m :

The rock consists of medium-grained schist being composed of muscovite, biotite and quartz, accompanied by segregated quartz veins. Although the rock facies shows quartz > biotite ≧ muscovite in most part, a part showing biotite < muscovite is also found in the section between 73.00 m and 79.50 m. Chlorite schist or amphibole schist is intercalated in very limited parts between 30.33 ~ 31.60 m and between 37.70 ~ 38.55 m.

Below 21.50 m, pink garnet 0.50 to one centimeter across is found as porphyroblast.

99.00 ~ 103.50 m :

The rock consists of chlorite-biotite-quartz schist.

103.50 ~ 122.00 m :

The rock consists mainly of dark green schist characteristically accompanied by biotite and chlorite or amphibole. Abundant segregated quartz veins having been deformed and showing a patchy appearance are found in the rock.

Porphyroblasts of garnet begin to appear at the depth of 21.50 m are most abundant in this section.

122.00 ~ 146.00 m :

The section consists of plagioclase-chlorite-biotite-quartz schist, containing garnet and pale brown staurolite. Biotite-quartz schist is intercalated partly.

146.00 ~ 155.00 m :

The rock is composed of schist mainly consisting of muscovite, biotite and quartz, often showing a banded structure with the repetition of biotite concentrated parts and quartz concentrated parts.

Although porphyroblastic garnet becomes a little scanty in this section than the part shallower than 146.00 m, staurolite rather becomes abundant and is found commonly.

155.00 ~ 235.90 m :

Schist consisting of muscovite, biotite and quartz and the one consisting of amphibole, biotite and chlorite constitute an alternating bed-like structure with each unit several centimeters to several meters in thickness. Segregated quartz veins are found everywhere, which seems to show a closer paragenetic relation with the latter.

Porphyroblastic garnet gradually becomes scanty and staurolite can not be observed.

235.90～300.15 m :

The section is composed of dark gray schist consisting of muscovite, biotite and quartz, locally containing segregated quartz veins having been deformed and showing a patchy appearance. Schist consisting of biotite and chlorite is intercalated in very limited parts.

Porphyroblastic garnet is partly found though scanty in quantity, becoming a little abundant at the bottom of the hole.

Mineralization is very weak in general, and only dissemination of minute-grained pyrrhotite, pyrite and chalcopyrite is observed in several parts. The assay result of ore shows a low content of the elements.

(4) Geologic Structure of the Hole

Schistose structure is notable in the rock found in the hole. Although the angle between the schistosity plane and the axis of the core (hereinafter referred to as schistosity plane angle) is about 60 degrees and is almost constant, microfold structure of several centimeters to several tens centimeters is partly observed.

3–2–2 Geology and Mineralization of Hole MBP–2

(1) Location

The hole is situated along a tributary in the upper reaches of Corrego do Morrinho about 2.5 km to the west-southwest of the CPRM camp, on the western side of Morro do Acampamento, at the point E792.73 longitude and 8551.17 latitude.

(2) Surface Geology of the Surroundings

The geology of the area has been thought that the schistose rocks such as schist of the Pip_4 vxt_2 member, amphibolites of the Pip_3 formation and schist of the Pip_5 formation are successively found from the east to the west. The detailed geological survey of this year led to the assumption that the amphibolites would be the intercalated rocks in the Pip_4 vxt_2 member, and moreover, graphite-quartz schist was observed on the west of amphibolites. It is assumed from the geologic distribution that the eastern side of amphibolites dips eastward, and the western side westward.

Actually, the exposure is very poor because of covering of laterite and Canga, limonitized laterite, and sand and gravel, the geology in the surroundings (Fig. II–3–32) was estimated based on the occurrence of a great number of floats. Hence the details of geologic structure can not be made clear.

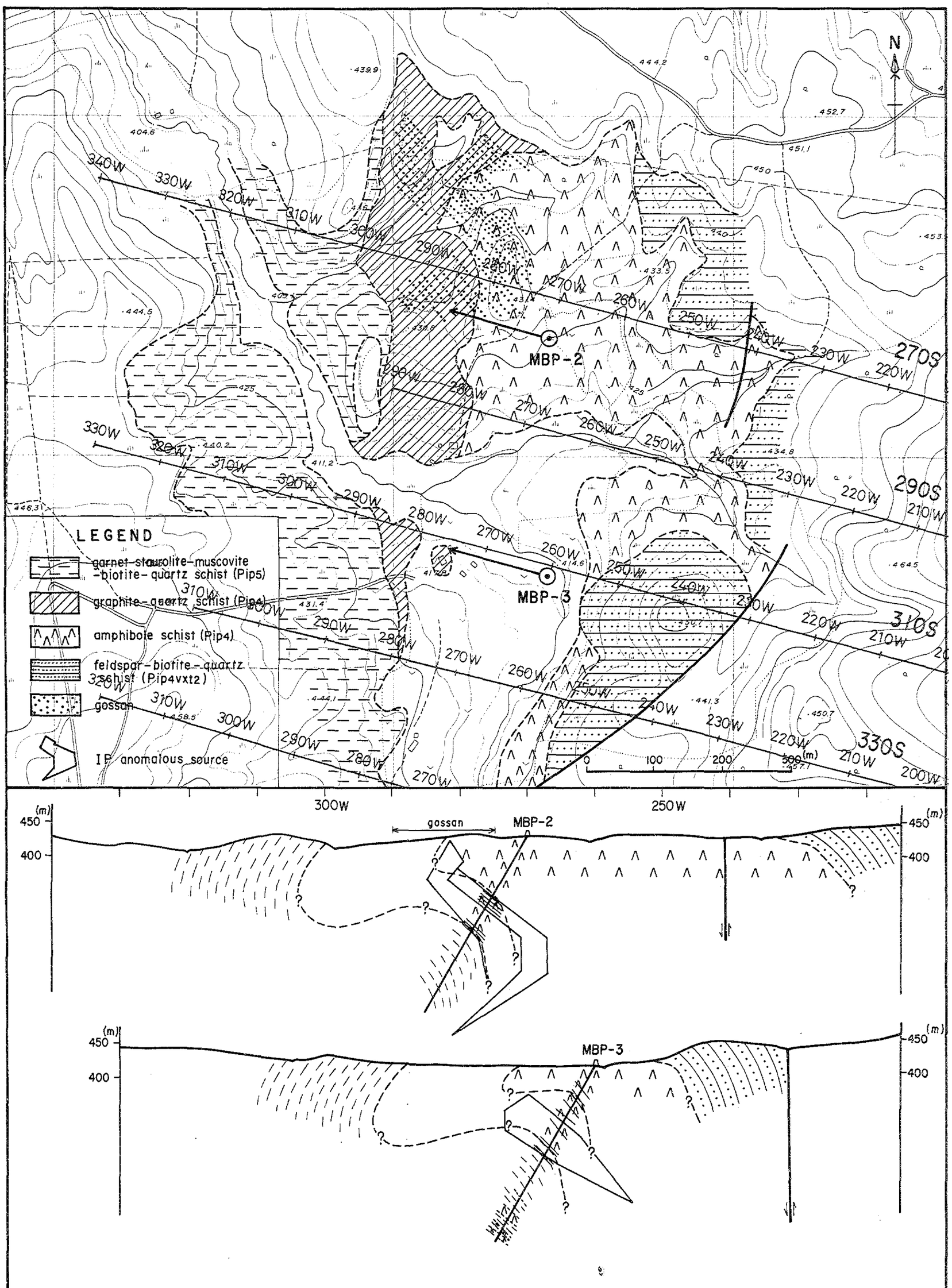

Fig. II-3-32 Geological Profile for MBP-2 and MBP-3

(3) Geology of Drill Hole

0.00 ~ 1.85 m :

The section consists of brown to reddish brown soil (A-horizon).

1.85 ~ 5.70 m :

The section consists of yellow to yellowish brown soil (B-horizon).

5.70 ~ 21.45 m :

The section of greenish gray and highly weathered fine grained rock (amphiblites?). The core was crashed to fine grains. The section up to 17.10 m is correlated to the C-horizon of the soil.

21.45 ~ 168.20 m :

The rock generally consists of chlorite-biotire-quartz-amphibole schist (amphibolites) showing a distinct schistosity. A part of chlorite shown in the columnar section was revealed from the result of microscopic observation to be the aggregate of chlorite, epidote and amphibole. It may be possible that the quantity of chlorite would have been exaggerated in the field.

Graphite-quartz schist of several centimeters to several meters in thickness is contained in the sections between 99.50 m and 120.50 m and between 160.00 m and 168.20 m. Pyrrhotite and pyrite are observed throughout the rock along the schistosity, which are most abundant in the section between 120.50 m and 168.20 m. The assay result of ores showed that Cu, Zn and S took the maximum values. Beside pyrrhotite and pyrite, chalcopyrite is observed under the microscope.

168.20 ~ 300.12 m :

Garnet and staurolite are contained as porphyroblasts, and the rock consists of muscovite-biotite-quartz schist often intercalated with lenticular quartz 10 to 20 centimeters thick. Pyrrhotite and pyrite show a rapid decrease, and chalcopyrite is very small in quantity though a little abundant than in the upper part.

(4) Geologic Structure of Drill Hole

The schistosity plane angle is a little higher than those of the Hole MBP–1, and is stable at around 70°.

3–2–3 Geology and Mineralization of Hole MBP–3

(1) Location

The hole is located at a point 350 m to the south of the Hole MBP–2, at E792.73 longitude and N8550.82 latitude.

(2) Surface Geology of the Surroundings

Although the geology is similar to that of Hole MBP–2, the distribution of amphibolites and graphite-quartz schist is narrower.

(3) Geology of Drill Hole

0.00 ~ 0.85 m :

The section consists of dark brown soil (A-horizon).

0.85 ~ 2.75 m :

The section consists of brown soil (B-horizon).

2.75 ~ 13.70 m :

The section consists of yellowish gray soil (C-horizon).

13.70 ~ 24.70 m :

The rock is gray and consists of highly silicified brecciated rock.

24.70 ~ 41.10 m :

The rock is a greenish gray metamorphosed rock and chlorite, quartz and calcite are observed under the microscope.

41.10 ~ 144.00 m :

The rock consists of chlorite-biotite-quartz-amphibole schist (amphibolites), and is massive below 113.30 m where no schistosity is observed.

Lenses or beds of graphite-quarts schist in the order of several to several tens centimeters reaching up to one meter in thickness are partly contained below 56 m. They are observed in large quantities in the section between 140.00 m and 143.60 m.

Also observed are pyrrhotite and pyrite associated with quartz vein, and dissemination of these is found along the schistosity. The content of Zn and S shows the maximum values in this section as in Hole MBP–2.

144.00 ~ 225.50 m :

The rock consists of muscovite-biotite-quartz schist containing porphyroblasts of garnet and staurolite.

Graphite-quartz schist accompanied by pyrrhotite and pyrite is intercalated in the section between 157.10 m and 162.50 m.

While disseminated chalcopyrite increases from 144.00 m toward the bottom of the hole, the dissemination of pyrrhotite and pyrite decreases. Beside these, cubanite, mackinawite, pentlandite and sphalerite are observed characteristically under the microscope.

225.50 ~ 251.00 m :

The section consists of biotite-quartz schist containing chlorite.

252.00 ~ 264.50 m, 280.00 ~ 284.00 m and 286.50 ~ 295.00 m

These sections are composed of biotire-quartz-amphibole achist.

264.50 ~ 280.00 m, 284.00 ~ 286.50 m, and 295.00 ~ 300.10 m

These sections are composed of garnet-staurolite-muscovite-biotite-quartz schist.

(4) Geologic Structure of Drill Hole

Although the schistosity plane angle is relatively stable, being 70° to 80° in general, it shows an acute angle of 40° at the depth of around 35m. In the section between 113.30 m and 140.00 m, the rock is massive and no notable schistosity is observed.

3–3 Discussion

3–3–1 Discussion on Results of Geophysical Survey

The interpretation result of geophysical survey (SIP electrical method) is not an absolute solution of geological structure for mineral exploration. Then, the integrated interpretation using the results of several and different geophysical methods should be done to evaluate the target area. And, if new information like the drilling survey results, etc. could be obtained, the geophysical method will present the basic data to understand more clearly the underground structure by the re-interpretation work of the survey data obtained formerly.

Taking into consideration of the above, the summary and consideration of the geophysical survey results are described as follows:

Apparent resistivities in this survey area show clear distribution pattern; the high zone of higher than 1,000 ohm-m at the Morro do Acampamento, and the apparent resistivity zone of less than 1,000 ohm-m at its surrounding area. And at the boundaries between both zones there can be seen strong resistivity contrasts which suggest the existence of the geological boundaries and/or fault structures. As iso-apparent resistivity lines in N-S direction are predominantly distributed, the resistivity structure with N-S trend are dominated in this survey area.

Promising IP indications (IP anomalous zones) show the spectral patterns due to sulfide minerals, and show the distribution pattern caused by N-S trending anomalous source. However, it is very difficult to discriminate particularly the content of pyryte and chalcopyrite only from the spectral patterns observed.

The drilling survey was conducted at three locations, the MBP-1 hole in the Block North, and the MBP-2 and the MBP-3 holes in the Block South, which were decided from the interim results of the SIP electrical survey.

(1) Block North

Lines 130S and 150S, overlapped 500m length each to the lines of the last phase, were measured again to confirm the IP anomalous zone detected by the last SIP electrical survey. As a result, the whole distribution and the characteristics of IP anomalous zone were clearly understood.

Apparent resistivities show the distribution reflecting the geological structure with N-S trend. High apparent resistivities of higher than 1,000 ohm-m are widely distributed below −100 mGL (Ground Level), and increase those distribution area with depth. However, those are divided into two zones at −200 mGL:

1) One high apparent resistivity zone is found at the western part of the block, and becomes more broad toward south. Its distribution area almost coincides with that of Pip_4 vxt_2 layer distributed at the Morro do Acampamento. This layer, showing higher resistivity than other schist, seems to contain a lot of quartz.

2) Another zone is distributed in the depth at the eastern part of the area and may correspond to Pip_4 vxt_2 layer containing quartz locally.

Medium apparent resistivities from 500 to 1,000 ohm-m may correspond to the Pip_4 vxt_1 layer and amphibolites of the Pip_3 layer, and judging from those distribution pattern, these layers and/or rocks seem to be distributed broadly to the north beyond the survey area.

Low apparent resistivities of lower than 500 ohm-m show the distribution corresponding to the Pip_4 vxt_1 layer and may reflect strong weathered mica-quartz schist, except for the effect of the local low-resistivity layer at the shallower depth.

IP indications are found in the distribution area of the Pip_4 vxt_2 layer and of the Pip_4 vxt_1 layer containing locally quartz, and show spectral type (Type B) due to a small amount of sulfide minerals. These sulfide minerals seem to be the dissemination type in the whole area, judging from the distribution pattern of IP indications. And near the Line 150S, another IP indications expected to reflect the concentration of sulfide minerals, are found. By means of 2-D model analysis for these IP indications, two IP anomalous source, that is, two concentrations of sulfide minerals, are infered:

Anomalous source I;

This source shows east-dipping from the surface to the depth and IP effect of more than 3.0%.

Anomalous source II;

This is distributed at two portions, at the shallower part above −70 mGL and at the depth below −150 mGL, and is surrounded by the sulfide dissemination indicating the weak IP effect. The deeper source shows IP effect of 4.0%.

Taking into consideration of geological conditions, the drilling survey and the 2-D model analysis results, it is concluded that IP indications detected at Line 150S are caused mainly by the anomalous source II showing the spectral pattern of Type B.

The shallower one of the anomalous source II is distributed in the high resistivity zone near the Line 150S, but disappears and changes its spectral pattern to local Type C at Line 160S. While, the deeper one, showing east-dipping, may extend to the depth southward but no extension would be expected northwards.

(2) Block South

This block has been selected by the results of geochemical and geophysical (CSAMT method) surveys in the last phase.

Apparent resistivities are clearly classified into three zones, namely high, medium and low apparent resistivity zones. High and medium zones are found at the Morro do Acampamento and at the western foot of the Morro do Accampamento, respectively, and low zone is distributed at the western part of the block. These zones are arranged in N-S direction, so it is said that apparent resistivity distribution clearly reflects the geological structure with N-S trend in the area.

High resistivity zone seems to be a southern extension of high apparent resistivity zone in the Block North, and becomes wider towards south.

Medium zone reflects amphibolites. Judging from the SIP survey results, the amphibolites show the west-dipping between Lines 270S and 310S, and the east-dipping at the south of the Line 330S, so the folding structure is infered in this block.

Low zone corresponds to graphite quartz-schist. It shows west-dipping at the shallower part and east-dipping at the deeper part, so the zone also reflects the geological structure.

Two IP indications were distributed in this block; one is found in the distribution area of Pip_4vxt_2 layer containing a lot of quartz found at the Morro do Acampamento, and another one in the apparent resistivity zone of 100 to 300 ohm-m at the western ends of the Lines 270S, 310S, 330S and 350S. The former show a spectral pattern of Type B due to sulfide dissemination, and the latter show Type A with a strong IP effect due to graphite-quartz schist and sulfide minerals.

It has been thought that if graphite-quartz schist is distributed at gentle west-dipping like the distribution of low resistivity layer of less than 100 ohm-m, sulfide minerals would exist strati-

formly in amphibolites below graphite quartz-schist. However, a spectral pattern of Type A seems to reflect both of graphite quartz-schist and sulfide minerals, so it was understood that graphite quartz-schist may exist in amphibolites. Moreover, the effect of graphite quartz-schist for a spectral pattern can be seen more remarkably in the depth and graphite quartz-schist also affects the IP effect, in particular, the magnitude of the IP effect in the depth of the Block South. It is expected that the IP anomalous source in the Block South would show higher value than that detected near Line 150S in the Block North, because the source in the South corresponds to compact sulfide dissemination and graphite quartz-schist and that in the North due to the dissemination of a small amount of sulfides. However, P.F.E. in both blocks show almost the same values, and the spectral patterns at the shallower part of the South are similar as those of the North, in spite of different geological conditions and different strength of the mineralization in both blocks. The reason is as follows:

1) The IP anomalous source in the Block North corresponds to a small amount of sulphide minerals distributed homogeneously, a small-scale source at the shallower part and/or that distributed horizontally in the depth. On the other hand, the IP anomalous source reflects the effect of the negative coupling originating in the geological environment, or the combined effect of graphite quartz-schist and sulphide minerals. Therefore, P.F.E. in both blocks show almost the same values.

2) The similarity in the spectral patterns of both blocks may be seen because both sources are due to sulfide disseminations.

(3) IP Anomalies and Drilling Survey Results

The MBP-1 hole, drilled on Line 150S where the concentration of sulfide minerals might be expected, hit the pyrite dissemination and not the ore body. Then, judging from the drilling survey result and the characteristics of IP anomaly, it is thought that IP anomalous source detected near Line 150S are considered to be due to lateral effect of sulphide dissemination on Line 160S.

Two holes, MBP-2 and MBP-3, were drilled in the SIP anomalous zone, which is thought to be due to graphite quartz-schist with west -dipping at the shallower depth and due to sulfide minerals with east-dipping in the depth. The target of drilling survey was a deeper source.

As a result of the drilling survey, the IP anomalous source corresponds to sulfide minerals (pyrrhotite and pyrite) concentration and graphite quartz-schist with the thickness of 70m in the MBP-2 hole. At the concentration of the sulfide minerals, a small content of chalcopyrite is contained, and chalcopyrite increases its content with depth. The MBP-3 hole hit the sulfide minerals and graphite quartz-schist with the thickness of about 100m. These IP anomalous

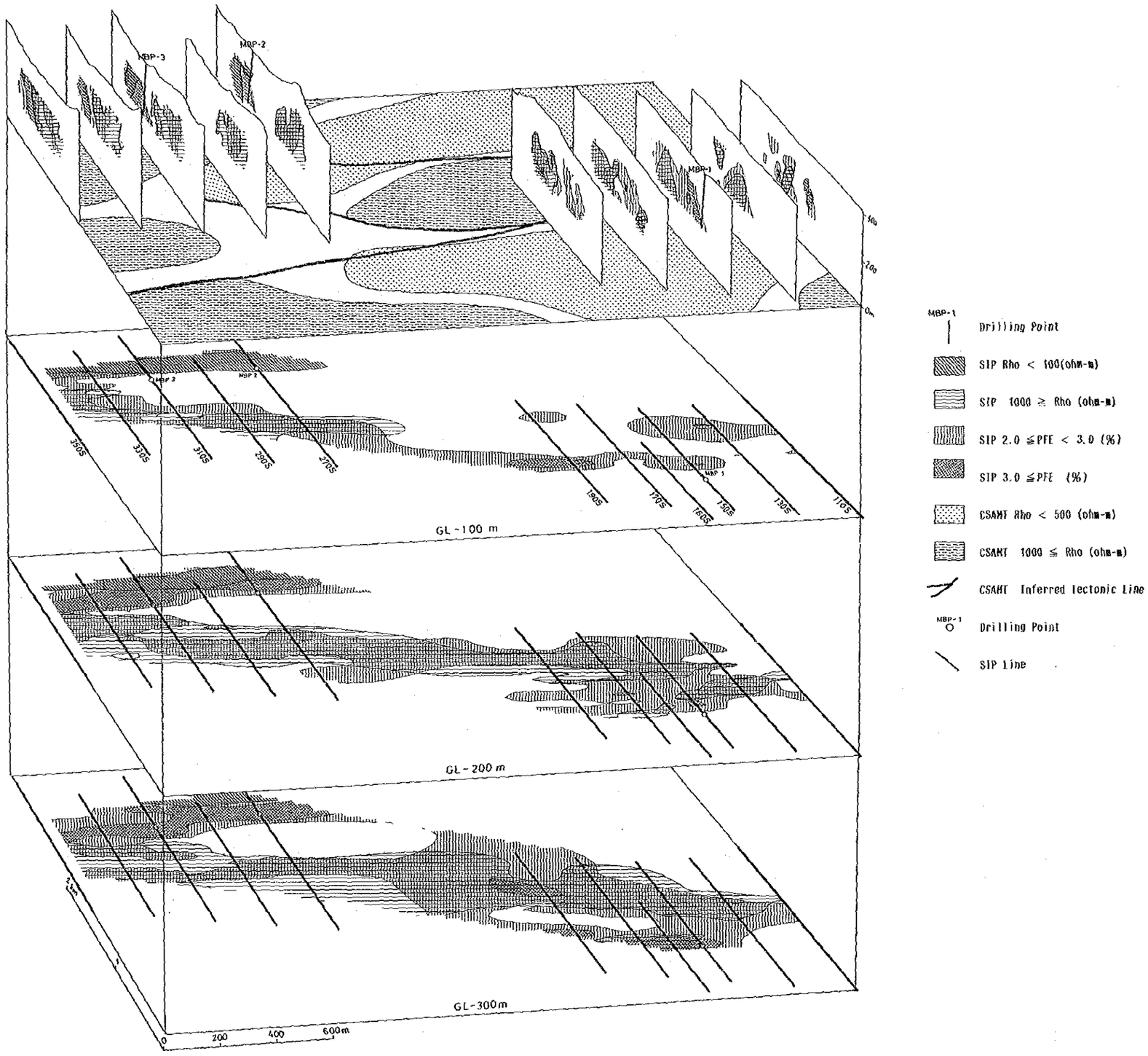

Fig. II-3-33 SIP Interpretation Map

sources, hit in both holes, exist in the same horizon, according to the results of the 2-D model analysis. However, the both holes could not hit the ore body. The reason is described below.

1) It was impossible to discriminate the minerals and/or ore bodies because the spectral patterns observed reflect both of graphite quartz-schist and sulfide mineral dissemination. However, core samples show high P.F.E. values according to the results of the physical property measurement.

2) Even if there exists the sulfide ore deposit, it would be a small-scale in size, so it seems to be difficult to decide the drilling locations.

In this SIP electrical survey, although it was failed to hit the ore body, the geological structure in the area and the characteristics and distribution of the IP anomalous sources was clarified.

3–3–2 Discussion on the Results of Drilling Survey

(1) Hole MBP–1

Although it is difficult to determine whether chlorite-biotite-amphibole schist in the section between 103.50m and 122.00m belongs to the intercalated bed in the $Pip_4 vxt_1$ member or to the amphibolites of the Pip_3 formation, the former interpretation appears more appropriate judging from the facts that the geological data of the surroundings show that the thickness of the bed is thin and that quartz and biotite are more abundant in the rock than Pip_3 formation.

The assay result of the drill core shows that the content of sulfide minerals is less than one percent. The test of physical properties showed a low value of PFE, and no phenomenon corresponding to the IP anomaly has been grasped. This is inconsistent with the data obtained in the geophysical survey carried out on the surface. Because of dependence of the present method of interpretation on the 2–dimensional model, it is highly possible that the anomalous source detected in the neighborhood of the survey line would be interpreted as a anomalous source immediately below the survey line. In the case of this hole, it is very difficult to make 3–dimensional interpretation, but it may be possible that there is some anomalous source on the southern side of the survey line 150S.

(2) Holes MBP–2 and MBP–3

As a result of the surface geological survey, it was at first interpreted that the geologic structure on the western side of the drill holes would show a gentle dip toward the west.

The geophysical survey led to detect an anomaly consistent with graphite bearing quartz schist at a shallow part near the surface and an east-dipping anomaly in the deeper part of the amphibolites. Although whether these anomalies are of different sources or belong to a continuous system was not clear, the model interpretation show that they belong to the same anomal-

PART III CONCLUSION AND RECOMMENDATION

CHAPTER 1 Conclusion

1–1 Rio Dois De Junho Area

A sporadical geochemical anomalous zone of Cu-Pb-Zn was extracted in the southern portion of the area. However it seems difficult to expect ore deposits of the same type of the Palmeirópolis'. Even if existed, it is presumed to be of a small scale.

1–2 Morro do Acampamento Area

(1) The hole (MBP-1) was drilled in order to confirm the IP anomaly which was detected below around the point 85W of line 150S in the Block North. But no remarkable mineralization was intersected.

(2) Strong IP anomalies with almost the same magnitude as ones of C-1 deposit, and trending N-S, were detected in a low to middle resistivity zone in the Block South.

(3) In order to confirm the IP anomalies between points of 270W and 280W of line 270S, and between points of 260W and 270W of line 310S, the drillings of MBP-2 and MPB-3 were conducted. As a result, dissemination of sulphide minerals (mainly composed of pyrite and pyrrhotite) with a maximum weight percent of 7 and thin layers of graphite-quartz schist, were intersected in amphibolites, with widths of 70m and 100m, but useful minerals such as chalcopyrite were found a little.

CHAPTER 2 Recommendation for Phase III Survey

The graphite-quartz-schist intersected by the drillings in the Block South is probably correlated with the iron formation overlying the C-2 and C-3 ore deposits, so that there is still a possibility that the ore horizons of the C-2 and C-3 deposits may exist in the Block South.

As the Alvo 10P area has not provided us enough information from the depth though many informations on geochemical, geophysical (IP), and shallow drilling data have been obtained through CPRM, follow-up surveys to collect information from the depth are expected.

Therefore, in Phase III, the following follow-up surveys are recommended to be carried out in the Morro do Acampamento area.

(1) Drilling for the final evaluation of the Block South.

(2) Geophysical SIP survey and Drilling for collection of informations at depths in the Alvo 10P area.

LIST OF ILLUSTRATIONS

LIST OF TABLES

LIST OF APPENDICES

LIST OF PLATES

REFERENCES

(1) Almeida F.F.M., Hasui Y., Brito Neves B.B. and Fuck R.A. – 1981 – Brasilian structural provinces; an introduction, Earth-Sci., Rev., 17: 1-29.

(2) Almeida F.F.M. e Hasui, Y. – 1984 – O Precambriano do Brasil.

(3) CNEN/DNPM/CPRM – 1973 – Levantamento Aerocintilometrico Projecto Serra da Mesa.

(4) CNEN/DNPM/CPRM – 1977 – Projeto Serra da Mesa II-Goias, Relatorio Final.

(5) CPRM – 1984 – Projeto Plameirópolis Informe Tecnico.

(6) DNPM – 1975 – Carta Geologica do Brasil ao Miliodesimo, Folha Goias SD-22.

(7) DNPM/MME – 1981 – Projeto RADAMBRASIL, Vol. 25.

(8) DNPM – 1981 – Geologia e Inventario dos Recursos Minerais do Regiao Central do Estado de Goias – Projeto Brasilia –.

(9) DNPM – 1981 – Os Principais Depositos Minerais do Regão Centro-Oeste.

(10) DNPM – 1983 – Levantamento Aerogiofisico do Projeto Palmeiropolis-GO.

(12) DNPM – 1983 – Garimpos do Brasil.

(13) DNPM – 1984 – Garimpos do Brasil.

(14) DNPM – Projeto Mapas Metalogeneticos e de Previsão de Recurais Minerais – Porangatu – Folha SD-22-X-D.

(15) DNPM – Projeto Mapas Metalogeneticos e de Previsão de Recurais Minerais – Alvorada – Folha SD-22-X-B.

(16) Girardi A.V. and Kurat G. – 1982 – Precambrian Mafic and Ultramfic Rock of the CANABRAVA Complex, Brasil.

(17) Hasui Y. et al. – 1980 – Datacoes Rb-Sr e K-Ar Centro Norte do Brasil e seu Significado Geologico-Geotectonico, XXXI Congresso Brasileiro de Geologia.

(18) Louis L. – 1978 – Aspectos Geotectonicos da Africa Ocidental a Leste do Golfo da Guine com Refrencia as Conexoes Estruturais e Litoloficas Brasil e Africa, XXX Congresso Brasileiro de Geologia.

(19) Ishikawa, H., Sawaguchi, T., Iwaya, S. and Horiuchi, M. – 1976 – Delineation of Prospecting Targets for Kuroko Deposits Based on Modes of Volcanism of Underlying Dacite and Altoration Haloes, Mining Geology, 26, 105-117 (abstract in Japanese)

(20) Meyers, R.E. and MecLean, W.H. – 1983 – The geology of the New Inco copper deposit, Norana district, Quebec, CAN. J. EARTH SCI., Vol. 20, 1291-1304.

(21) MMAJ – 1985 – Report on Morro Agudo and Palmeirópolis Project, Brasil.

(22) Severin, P.W.A. -- 1982 -- Geology of the Sturgeon Lake Copper-Zinc- Lead-Silver-Gold Deposit, CIM. Bull., Vol. 75, 107-123.

(23) Sinclair, A.J. -- 1974 -- Selection of Threshold Values in Geochemical Data Using Probability Graphs, J. Geochem. Explor., 3, 129-149.

(24) Suszczynski E. -- 1981 -- South America, Structural Framework, Chapter 13 of Precambrian of the Southern Hemisphere.